



**Politecnico  
di Torino**

**Politecnico di Torino**

Master degree in Sustainable Nuclear Energy

**Stochastic Methods for the  
Solution of the Adjoint Transport  
Equation**

**Candidate:**

Simone Occhipinti

**Supervisors:**

Prof. Sandra Dulla

Dr. Nicolò Abrate

Academic Year 2024/2025

# Contents

<b>1</b>	<b>Preface</b>	<b>5</b>
<b>2</b>	<b>Introduction</b>	<b>7</b>
2.1	Neutron transport theory . . . . .	7
2.2	Monte Carlo methods . . . . .	9
2.3	Neutron importance . . . . .	11
<b>3</b>	<b>Direct and adjoint transport</b>	<b>13</b>
3.1	Monte Carlo solution of the adjoint transport equation . . . . .	13
3.2	Sampling procedure . . . . .	15
3.3	Adjoint transport phenomena . . . . .	20
<b>4</b>	<b>An in-house Monte Carlo code</b>	<b>25</b>
4.1	Generalities . . . . .	25
4.2	Particle sampling . . . . .	27
4.3	Free flight sampling . . . . .	32
4.4	Energy sampling . . . . .	38
4.5	Variance reduction techniques . . . . .	40
4.6	Population control techniques . . . . .	41
4.7	Scoring . . . . .	43
<b>5</b>	<b>Code verification</b>	<b>46</b>
5.1	Problem definition . . . . .	46
5.2	Direct Placzek problem . . . . .	48
5.3	Adjoint Placzek problem . . . . .	49
5.4	Statistical reliability of the results . . . . .	54
<b>6</b>	<b>Conclusions</b>	<b>58</b>

*CONTENTS*

2

**A The adjoint operator**

**61**

# List of Figures

3.1	Adjunctons scattering multiplicity, value refers to $U^{234}$ and $U^{238}$ are increased and decreased by a factor of 10 respectively. . . . .	22
3.2	Neutron and adjuncton energy emission spectrum . . . . .	24
3.3	Neutron and adjuncton number of particle emitted per fission . . . . .	24
4.1	Monte Carlo code flow chart . . . . .	26
4.2	Comparison between adjoint fission spectrum and sampling functions	31
4.3	Comparison between rejection methods performance . . . . .	31
4.4	Test on interface treatment, Neutrons . . . . .	36
4.5	Test on interface treatment, Neutrons . . . . .	36
4.6	Test on interface treatment, Adjunctons . . . . .	37
4.7	Test on interface treatment, Adjunctons . . . . .	37
5.1	Analytical and simulated results of direct slowing down problem, A=5, N=10 <sup>5</sup> . . . . .	50
5.2	Analytical and simulated results of direct slowing down problem, A=10, N=10 <sup>5</sup> . . . . .	50
5.3	Analytical and simulated results of direct slowing down problem, A=20, N=10 <sup>5</sup> . . . . .	50
5.4	Analytical and simulated results of direct slowing down problem, A=8, N=10 <sup>5</sup> . . . . .	50
5.5	Analytical and simulated results of direct slowing down problem, A=15, N=10 <sup>5</sup> . . . . .	50
5.6	Analytical and simulated results of direct slowing down problem, A=25, N=10 <sup>5</sup> . . . . .	50
5.7	Analytical and simulated results of adjoint slowing down problem, A=5, N=10 <sup>5</sup> . . . . .	53

5.8	Analytical and simulated results of adjoint slowing down problem, A=10, N=10 <sup>5</sup> . . . . .	53
5.9	Analytical and simulated results of adjoint slowing down problem, A=20, N=10 <sup>5</sup> . . . . .	53
5.10	Analytical and simulated results of adjoint slowing down problem, A=8, N=10 <sup>5</sup> . . . . .	53
5.11	Analytical and simulated results of adjoint slowing down problem, A=15, N=10 <sup>5</sup> . . . . .	53
5.12	Analytical and simulated results of adjoint slowing down problem, A=25, N=10 <sup>5</sup> . . . . .	53
5.13	Comparison of FOM values for different weight windows . . . . .	57

# Chapter 1

## Preface

The following work attempts to enumerate and investigate a rather large number of issues related to the stochastic solution of the adjoint neutron transport equation. This is a crucial argument in the field of nuclear reactor physics, since the adjoint flux distribution coincides with the importance distribution, and both play an important role in the design of a nuclear core. Importance is a measure of how much a particle contributes to the state of the system. The first application of this concept was in the formulation of Generalised Perturbation Theory, where studies of control rod positioning and movement showed that the importance of the absorbed neutrons was the most important parameter in evaluating the control rod effect. Similarly, reactor kinetic parameters are strongly influenced by the importance distribution: i.e. in a thermal reactor the effective delayed neutron fraction is higher than in a fast reactor, even though they may have the same fuel.

This equivalence has led to the possibility of avoiding deterministic approaches to the calculation of importance, so that the same MC code can be used to simulate both direct and adjoint transport. This goal became particularly interesting when considering that MC codes are the most widely used and optimised approach to solving the Boltzman equation. In addition, zero-variance MC methods require prior evaluation of the importance distribution to increase the accuracy of the results. Therefore, the ability to perform a single simulation, rather than a hybrid between deterministic and stochastic solutions, can lead to the development of powerful tools for nuclear engineering.

In order to accomplish this task, some basic knowledge is first introduced to provide

a useful background for future argumentation. The relationship between direct and adjoint transport is then explored: the introduction of a new type of particle requires the derivation of its transport properties. From this, the procedure for simulating an adjoint random walk is outlined. The main part of the thesis is devoted to the presentation of an in-house MC code developed to solve both direct and adjoint transport problems. Within Chapter 4, all the sampling functions implemented are described, coupled with how corrections would be applied to better handle adjoint transport. To ensure the reliability of the results, the well-known case study of the deceleration problem is analysed.

# Chapter 2

## Introduction

### 2.1 Neutron transport theory

Nuclear reactor physics was born during the Second World War with the establishment of the Manhattan Project. The first applications were to understand and exploit the interactions between neutrons and matter. The first demonstration of the possibility of achieving a positive net energy balance by controlling a fission chain reaction was Fermi's pile. This is the ancestor of the nuclear power plant core and, despite its simplicity of design, meets all the requirements of a nuclear reactor. From there, the applications of nuclear technology expanded to include transport, medicine, space travel and more.

The milestone of all activities related to the nuclear field is the Boltzman neutron transport equation [1]:

$$\begin{aligned} \Omega \cdot \nabla \phi(\vec{r}, E, \vec{\Omega}) = & -\Sigma_t(\vec{r}, E)\phi(\vec{r}, E, \vec{\Omega}) + \\ & + \oint_{4\pi} d\vec{\Omega}' \int_0^\infty dE' \Sigma_s(\vec{r}, E') f_s(\vec{r}, E', \vec{\Omega}' \rightarrow E, \vec{\Omega}) \phi(\vec{r}, E, \vec{\Omega}) + \\ & + \frac{1}{K} \frac{\chi(E)}{4\pi} \oint_{4\pi} d\vec{\Omega}' \int_0^\infty dE' \nu_f(\vec{r}, E') \Sigma_f(\vec{r}, E') \phi(\vec{r}, E', \vec{\Omega}). \end{aligned} \quad (2.1)$$

This equation describes the neutron distribution in a multiplicative and stationary system. The unknown is the neutron flux, defined as the product of the particle density and its velocity,  $\phi(\vec{r}, E, \vec{\Omega}) = v(E)\psi(\vec{r}, E, \vec{\Omega})$ . The collection of all independent variables,  $(\vec{r}, E, \vec{\Omega})$ , is called the phase space and can be defined as the domain of existence of the equation. On the other hand, a more practical point of view can

help to grasp the reason for all the variables used: moving from the density distribution to the single particle, the transport phenomenon can be described in terms of its position,  $\vec{r}$ , and its velocity,  $\vec{v}$ . The latter is not explicit in the equation (2.1), but it is only necessary to decompose the vector  $\vec{v}$  into its magnitude,  $|v|$ , and direction,  $\vec{\Omega}$ . Finally, the magnitude is expressed as a function of energy using the definition of kinetic energy. Often the dependence on the direction of flight is neglected, so the problem is written in terms of the scalar flux,  $\Phi(\vec{r}, E) = \oint_{4\pi} d\vec{\Omega} \phi(\vec{r}, E)$ .

A brief description of each phenomena involved is provided.

- $\Omega \cdot \nabla \phi(\vec{r}, E, \vec{\Omega})$

The streaming term represents the spatial motion of the particles. This means the net balance of neutrons passing through the observed volume of space, so it can be generally referred to as the 'leakage' term.

- $\Sigma_t(\vec{r}, E)\phi(\vec{r}, E, \vec{\Omega})$

The removal term counts the fraction of particles initially inside the observed phase volume that change their energy or direction as a result of a collision. Here the unit of the equation (2.1) can be easily explained:  $\Sigma_t(\vec{r}, E) \left[ \frac{1}{cm} \right]$  is the probability per unit path to have an interaction, while  $\phi(\vec{r}, E, \vec{\Omega}) \left[ \frac{1}{cm^2 eV s} \right]$ , so the result is the collision density normalised to the phase volume  $F(\vec{r}, E, \vec{\Omega}) \left[ \frac{1}{cm^3 eV s} \right]$ .

- $\oint_{4\pi} d\vec{\Omega}' \int_0^\infty dE' \Sigma_s(\vec{r}, E') f_s(\vec{r}, E', \vec{\Omega}' \rightarrow E, \vec{\Omega}) \phi(\vec{r}, E, \vec{\Omega})$

The scattering term counts the fraction of particles reaching the observed phase volume that change energy or direction as a result of scattering.  $f_s(\vec{r}, E', \vec{\Omega}' \rightarrow E, \vec{\Omega})$  is known as the scattering function and introduces the probability that a particle colliding within  $d\vec{r}dE'd\vec{\Omega}'$  will end up within  $d\vec{r}dEd\vec{\Omega}$ . Note that the integrals are used to account for all possible incoming energies and directions, including the observed one.

- $\frac{1}{K} \frac{\chi(E)}{4\pi} \oint_{4\pi} d\vec{\Omega}' \int_0^\infty dE' \nu_f(\vec{r}, E') \Sigma_f(\vec{r}, E') \phi(\vec{r}, E', \vec{\Omega})$

The fission term counts all neutrons produced by fissions within the observed phase volume.  $\nu_f(\vec{r}, E')$  is the number of neutrons produced by a reaction at energy  $E'$ , so the multiplicity depends on the pre-collision characteristics. On the other hand, the probability of emitting a neutron within  $dE d\vec{\Omega}$  is  $\frac{\chi(E)}{4\pi}$ . One last consideration must be spent to describe the term  $\frac{1}{K}$ : it is an artificial degree of freedom introduced to ensure a meaningful solution of the equation. Physically, it describes how far the system goes before going critical.

A more general form of the equation (2.1) also includes a source term,  $S(\vec{r}, E, \vec{\Omega})$ , which is nothing more than an external positive contribution that can be arbitrarily defined. In the case discussed here, the fission term plays the role of the source.

In order to pose the problem well, it is necessary to define boundary conditions. Most applications can be resumed in the case of void boundary conditions: no incoming neutrons from outside the system.

$$\phi(\vec{r} = \vec{R}_{end}, E, \vec{\Omega} = \vec{\Omega}_{in}) = 0 \quad \forall E \quad (2.2)$$

where  $\vec{R}_{end}$  is a short notation to indicate all the edges of the domain, the same for  $\vec{\Omega}_{in}$  which includes all incoming directions.

## 2.2 Monte Carlo methods

Monte Carlo (MC) methods are a family of algorithms designed to reproduce the results of physical experiments on a computer. Their aim is to simulate stochastic phenomena by sampling random numbers: often complex systems can be decomposed into a subset of different random processes with known probability density functions (PDFs). MC codes were born and developed alongside nuclear physics during the Manhattan Project. Metropolis, Ulam and von Neumann were pioneers in applying probabilistic approaches to a wide range of problems, as can be seen in the paper by Metropolis and Ulam [2]. They were able to perform the first MC simulation of a thermonuclear reactor on ENIAC, the first computer ever built. The accuracy of the results obtained marks a turning point in the history of reactor physics, since from that moment on interest in stochastic methods increased until they became a cornerstone of nuclear engineering knowledge. A very interesting

account of the history of the project was written by Metropolis [3].

Over time, the invention of more powerful computational tools and the development of optimisation techniques (i.e. parallelism) led to the consolidation of MC methods as the main solution to the neutron transport equation (2.1). Tripoli-4 [4] is the MC code released by the CEA in the 1990s, which has high accuracy results due to advanced variance reduction (VR) techniques. Another example is Serpent 2 [5], developed at the VVT Technical Research Centre and optimised for core design and fuel cycle studies. Finally, OpenMC [6] is an open source MC code that will be launched at MIT in 2011. In addition to availability, its main features are high parallelism to increase computational power and the potential to perform large-scale simulations.

After giving some references to reconstruct the state of the art of MC codes, it may be useful to give a very brief explanation of how they work. However, the argument will be discussed in detail later. Given a phase space consisting of  $N$  independent variables, a generic particle in it can be described by a vector of length  $N$ . After a certain time interval  $\Delta t$ , the properties of the particle change due to random processes (i.e. scattering), and the new values can be collected in a new vector of the same size. Thus, it can be assumed that there exists a set of probability distributions that can describe all possible outcomes depending on the initial conditions. For example, it has been shown that the jump between two different energy levels occurs as a random process. Thus, if we consider a sufficiently large number of particles at time  $t$  and perform this 'random application' on them, the law of large numbers ensures that we get a good approximation of how the particles will be distributed on average at  $t + \Delta t$ . Repeating this process for a sufficiently large number of time steps will lead to the stationary distribution, if it exists. The main feature of the MC code is thus the transition from complex integrals and probability matrices to a simple chain of random events; on the other hand, a huge number of histories is often required.

## 2.3 Neutron importance

The concept of neutron importance was first introduced by A. M. Weinberg and E. P. Wigner [7] as a measure of how significantly a single neutron can influence the state of a chain reactor. The definition comes from the application of perturbation theory to nuclear design to assess the effect of the presence of control rods and the parameters on which it depends. An opposite point of view may be clearer, without any lack of completeness: the introduction of an external neutron into a critical system results in an increase of the neutron population. The number of descendants supplied to the reaction can be interpreted as how 'important' the ancestor is to it.

Once a general definition is given, it is necessary to provide a tool that allows the evaluation of the importance distribution. From a mathematical point of view, the importance is a scalar property associated with neutrons that depends on their position in phase space,  $\psi(\vec{r}, E, \vec{\Omega})$ . So the value associated with a population of neutrons can be expressed as  $N_0 \cdot \psi(\vec{r}, E, \vec{\Omega})$ , where  $N_0$  is the particle density. As in the case of the equation (2.1), let's consider a multiplicative stationary system: since the importance of a neutron is proportional to the power it produces, it can be assumed that its progeny will have the same importance. Following the procedure described in Ussachoff's book [8], a balance equation for a group of particles travelling along a segment  $ds$  can be written as follows

$$\begin{aligned}
 N_0\psi(\vec{r}, E, \vec{\Omega}) &= N_0 (1 - \Sigma_t(\vec{r}, E)ds) \psi(\vec{r} + \vec{\Omega}ds, E, \vec{\Omega}) \\
 &+ N_0\Sigma_s(\vec{r}, E)ds \oint_{4\pi} d\vec{\Omega}' \int_0^\infty dE' f_s(\vec{r}, E, \vec{\Omega} \rightarrow E', \vec{\Omega}')\psi(\vec{r}, E', \vec{\Omega}') \\
 &+ N_0\frac{\nu(\vec{r}, E)}{K}\Sigma_f(\vec{r}, E)ds \oint_{4\pi} d\vec{\Omega}' \int_0^\infty dE' \frac{\chi(\vec{r}, E')}{4\pi}\psi(\vec{r}, E', \vec{\Omega}'). \quad (2.3)
 \end{aligned}$$

The left term is the total importance in the original position. Meanwhile, the right term is composed of three different contributions, in order: the importance transported by particles that do not interact, the importance transported by particles scattered in all possible phase volumes, and the importance transported by particles produced by fissions. Note that also in this case it is necessary to introduce the factor  $\frac{1}{K}$  to guarantee a nonzero solution. Each term is constructed by multiplying the neutron density,  $N_0$ , with the fraction of particles emitted in a chosen phase volume,  $\nu_k f_k(\vec{r}, E, \vec{\Omega} \rightarrow E', \vec{\Omega}')dE'd\vec{\Omega}'$ , and the probability to interact during the

displacement,  $\Sigma_k(\vec{r}, E)ds$ . The final goal may seem obvious: a partial differential equation for the importance.  $N_0$  can be simplified and some terms rearranged.

$$\begin{aligned} \psi(\vec{r}, E, \vec{\Omega}) - \psi(\vec{r} + \vec{\Omega}ds, E, \vec{\Omega}) &= -\Sigma_t(\vec{r}, E)ds\psi(\vec{r} + \vec{\Omega}ds, E, \vec{\Omega}) \\ &+ \Sigma_s(\vec{r}, E)ds \oint_{4\pi} d\vec{\Omega}' \int_0^\infty dE' f_s(\vec{r}, E, \vec{\Omega} \rightarrow E', \vec{\Omega}')\psi(\vec{r}, E', \vec{\Omega}') \\ &+ \frac{\nu(\vec{r}, E)}{K}\Sigma_f(\vec{r}, E)ds \oint_{4\pi} d\vec{\Omega}' \int_0^\infty dE' \frac{\chi(\vec{r}, E')}{4\pi}\psi(\vec{r}, E', \vec{\Omega}'). \end{aligned} \quad (2.4)$$

The last step is to divide for the movement,  $ds$ , and compute the limit for  $ds \rightarrow 0$ . On the left side the definition of the gradient computed along the direction of the displacement.

$$\begin{aligned} -\vec{\Omega} \cdot \nabla\psi(\vec{r}, E, \vec{\Omega}) + \Sigma_t(\vec{r}, E)\psi(\vec{r} + \vec{\Omega}, E, \vec{\Omega}) \\ = \Sigma_s(\vec{r}, E) \oint_{4\pi} d\vec{\Omega}' \int_0^\infty dE' f_s(\vec{r}, E, \vec{\Omega} \rightarrow E', \vec{\Omega}')\psi(\vec{r}, E', \vec{\Omega}') \\ + \frac{\nu(\vec{r}, E)}{K}\Sigma_f(\vec{r}, E) \oint_{4\pi} d\vec{\Omega}' \int_0^\infty dE' \frac{\chi(\vec{r}, E')}{4\pi}\psi(\vec{r}, E', \vec{\Omega}'). \end{aligned} \quad (2.5)$$

This is nothing more than the adjoint transport equation. The simplest boundary conditions to apply, and the most commonly used, are those related to the void. Again, defining the importance of a neutron as proportional to power, it can simply be assumed that the importance of outgoing neutrons is zero.

$$\psi(\vec{R}_{end}, E, \vec{\Omega}_{out}) = 0 \quad (2.6)$$

where  $\vec{R}_{end}$  is the position of the boundary and  $\vec{\Omega}_{out}$  is the direction normal to the outer surface.

A more rigorous derivations of the property of importance conservation, so also of the equation (2.5) can be found on the book by Lewin [9].

# Chapter 3

## Direct and adjoint transport

### 3.1 Monte Carlo solution of the adjoint transport equation

A more thorough perspective on the theoretical definition of importance has been provided by J. Lewin. The author first demonstrates the equivalence between the importance function and the adjoint with the aim of applying the variation principle and perturbation theory to a number of well-known case studies in reactor physics, the adjoint definition and properties can be found in his book [9]. This relationship allows the application of the importance principle to be extended to source-driven systems, thus decoupling it from fission and multiplicative media. According to this new view, it is necessary to redefine the concept of source of importance: when can a neutron be considered 'more important' than others? This crucial question points to the fact that there is no universal unit of measurement for the importance function; the role of a neutron within a given system can only be assessed in proportion to its peers. Thus, all importance values must be read as dimensionless numbers that can only acquire meaning when compared with others. Similarly, the importance function itself is related to the nature of the system: as mentioned above, the first definition was proportional to the neutrons produced, because of the deep focus on power generation; now it is possible to consider a study of the shielding capacity of a layer of concrete, where the most relevant characteristic is the probability of escape from the system. An equivalent but more rigorous formulation is given in Lewin's monograph, where he proves that, given a density function and the associated detector, the latter acts as a source term for the relative adjoint equation. Thus, the

importance is generated depending on how the neutrons are observed.

The generalisation of the importance definition greatly increases the number of possible applications rather than the design of nuclear power plants. Equally important is the relationship between the importance equation and the adjoint transport equation: the former is a property related to the neutrons it transports, while the latter has the same unit of measure as a particle density. Thus, the adjoint transport equation can be solved by MC simulations. According to the definition of the adjoint source, random walks start from the interaction of the neutrons with the detectors and move backwards in time until they cross the original source. This approach is particularly effective for calculations based on low-probability events. It is well known that for MC results the associated variance decreases with the square root of the number of histories performed, so the computational cost increases as the probability of a particle contributing to the sample decreases. For a sufficiently small detector (i.e. consider again the number of particles able to pass through a neutron shield), the computation can be very expensive and inefficient, since only a negligible fraction of the generated population will be able to complete the search. On the other hand, adjoint paths start from the detector and, if the source is large relative to the detector, almost all random walks will end there and contribute to the evaluation. The equivalence between the two estimated observables is guaranteed by the reciprocity theorem [9].

De Matteis [10] presents a method for sampling the adjoint transport equation based on the simulation of the random walk of artificial particles called "adjunctons". The idea behind this is to make standard MC codes capable of handling the adjoint equation: it is necessary to introduce the transport phenomena of adjunctons, and the most intuitive solution can be to describe them using the neutron data just implemented in existing codes. A later work [11] proposes to apply a direct equivalence between neutron and adjuncton cross sections, the main consequence being to define for the adjuncton the same types of reactions that are characteristic of neutrons: scattering, absorption and fission. Although this last consideration may seem quite intuitive, it is fundamental to note that the adjunctons have been defined arbitrarily, so that the description of the relative interactions is also arbitrary, as long as the reaction rate and the probabilities are preserved.

Saracco, Dulla and Ravetto [12] perform a series of MC simulations aimed at testing the sampling procedure proposed by A. De Matteis. The case study is the slowing down problem (i.e. the evaluation of the energy spectrum of neutrons in an infinite and homogeneous medium without absorption produced by a monoenergetic source). The solution is known as the Placzek function. The same case can be applied to the adjuncton: an analytical formulation is computed for the adjoint Placzek function and an analogue MC code is run to validate the sampling procedure. Furthermore, the increase in performance due to the application of VR techniques [13] is tested. It is found that scattering can increase the adjoint weight, potentially leading to large fluctuations at high energy, making both population control and particle splitting techniques results particularly efficient. It should be noted that scattering also increases the adjoint energy, so the term 'slowing down' does not have a direct physical implication as in the case of neutrons, but is retained for consistency.

## 3.2 Sampling procedure

Let's define a phase space with six independent variables: three space coordinates  $\vec{r}$ , energy  $E$  and two angles for the direction of flight  $\vec{\Omega}$ . A simplified version of the (2.1) can be written as [12]:

$$\begin{aligned} \vec{\Omega} \cdot \nabla \phi(\vec{r}, E, \vec{\Omega}) + \Sigma_t(\vec{r}, E) \phi(\vec{r}, E, \vec{\Omega}) = S(\vec{r}, E, \vec{\Omega}) \\ + \oint_{4\pi} d\vec{\Omega}' \int_0^\infty dE' \Sigma_t(\vec{r}, E') f(\vec{r}, E', \vec{\Omega}' \rightarrow E, \vec{\Omega}) \phi(\vec{r}, E', \vec{\Omega}'). \end{aligned} \quad (3.1)$$

Where  $f(f(\vec{r}, E', \vec{\Omega}' \rightarrow E, \vec{\Omega}))$  is known as total collision kernel and is a function describing all transport phenomena related to the system. Under the assumption of stationarity, the problem is guaranteed to be linear since the properties of the medium do not depend on the flux itself. Note that, to generalize the discussion also to non critical systems, the source term is included. Rewriting in the same way also the equation 2.5, two main differences can be highlighted: the sign of the streaming term and the 'direction' of the collision kernel.

$$\begin{aligned} -\vec{\Omega} \cdot \nabla \psi(\vec{r}, E, \vec{\Omega}) + \Sigma_t(\vec{r}, E) \psi(\vec{r}, E, \vec{\Omega}) = S^\dagger(\vec{r}, E, \vec{\Omega}) \\ + \oint_{4\pi} d\vec{\Omega}' \int_0^\infty dE' \Sigma_t(\vec{r}, E') f(\vec{r}, E', \vec{\Omega}' \rightarrow E, \vec{\Omega}) \psi(\vec{r}, E', \vec{\Omega}'). \end{aligned} \quad (3.2)$$

This can also be defined as the adjoint version of the equation (3.1). The former is the mathematical equivalent of the backward random walk performed by the adjoints: the direction of flight is reversed, so is the gradient. The latter underlines the difference between the derivation of the two equations and the different nature of the variables. The equation (3.1) is based on the conservation of mass, so its solution is representative of a density. Thus, the collision integral takes into account all the particles present in a different phase volume,  $\phi(\vec{r}, E', \vec{\Omega}') d\vec{r} dE' d\vec{\Omega}'$ , and multiplies it by the transfer function from their volume to the observed one,  $d\vec{r} dE d\vec{\Omega}$ . On the other hand, the equation (3.2) is derived from the importance balance, so the term represents the contribution of all possible outcomes produced by the neutron within  $d\vec{r} dE d\vec{\Omega}$ . It is important to stress that the importance is not a density, but a dimensionless quantity defined only as a ratio between neutrons: the fraction of scattered neutrons is calculated by  $\Sigma_t(\vec{r}, E') f(\vec{r}, E', \vec{\Omega}' \rightarrow E, \vec{\Omega})$  and multiplied by the importance after the collision. In summary, the direct collision term is based on pre-collision information, while the adjoint term is based on post-collision information.

The need to manage the equation (3.2) before attempting to solve it using an MC code has just been mentioned in the previous section. On the other hand, it may be useful to introduce a standard sampling procedure for direct MC simulation. Therefore, all the strategies to adapt it to the adjoint transport will be explained. The steps involved can be summarised as follows:

- **Birth:** sample the initial position, energy and direction of the particle from the source distribution;
- **Free-flight:** sample the distance travelled by the particle until it interacts, exponential distribution;
- **Interaction:** selects the type of interaction the particle will undergo and, if necessary, saves the fission site;
- **Outgoing data:** sample the new energy and direction after the collision;
- **Scoring:** collect the appropriate measure to estimate the flux;
- **Weight correction:** multiply the particle weight by the number of particles produced by the collision,  $\nu_k$ ;

- **Final check:** if the particle is still in the phase domain, restart from free-flight, otherwise end the story.

The procedure relates to an analogue MC code, but can also be used as a guide for a non-analog case. However, some care must be taken when evaluating the flux estimator and after applying the weight correction due to the implicit capture. A final step can be added before the final check to apply VR techniques. In order to properly sample the random variables depending on the random process, each physical process requires an associated PDF.

The most general way to derive a PDF from a source distribution is given by

$$f_S(\vec{r}, E, \vec{\Omega}) = \frac{S(\vec{r}, E, \vec{\Omega})}{\int_V d\vec{r} \oint_{4\pi} d\vec{\Omega} \int_0^\infty dE S(\vec{r}, E, \vec{\Omega})}. \quad (3.3)$$

The normalisation condition is naturally satisfied. In eigenvalue calculations, the source energy distribution must correspond to the fission spectrum, while the neutron emission can be assumed to be isotropic. The PDF associated with free-flight sampling can be derived from the probability that a particle interacts with the medium within a small interval  $dr$  after travelling a distance  $r$

$$p(r)dr = \Sigma_t e^{-\Sigma_t r} dr. \quad (3.4)$$

Where  $r = |\vec{r}|$ . In this case, the inverse transform method can be applied straightforwardly. For a more detailed discussion of standard MC procedures, the book by Haggihat [14] serves as a useful reference. Considering a set of reactions  $k = s, a, f$  (scattering, absorption, and fission) for neutrons, the total collision kernel can be expressed as done in the paper written by Saracco [12].

$$f(E', \vec{\Omega}' \rightarrow E, \vec{\Omega}) = \sum_{k=s,a,f} \frac{\Sigma_k(E')}{\Sigma_t(E')} \nu_k(E') f_k(E', \vec{\Omega}' \rightarrow E, \vec{\Omega}) \quad (3.5)$$

where  $f_k(E', \vec{\Omega}' \rightarrow E, \vec{\Omega})$  is the partial collision kernel, which defines the PDF governing the energy and angular distributions of the outgoing neutrons. From this,

the probability of encountering a particular type of interaction can be constructed

$$p_k(E) = \frac{\Sigma_k(E)}{\Sigma_t(E)}. \quad (3.6)$$

It is important to note that the partial collision kernels, as well as the total collision kernel, are normalised with respect to the outgoing energy and angle variables. This property may seem rather obvious, but it is a fundamental requirement for treating them as a PDF for sampling the neutron properties after the collision. The previous discussion of the scattering integral now has an active purpose for the construction of an adjoint random walk: it is not a PDF for the outgoing energy and angle, since it is normalised with respect to the incoming values. It is therefore necessary to construct an equation that is formally equivalent to the equation (3.5). The simplest approach is to define an adjoint total collision kernel

$$\Sigma_t(E)f(E, \vec{\Omega} \rightarrow E', \vec{\Omega}') = \Sigma_t^\dagger(E')f^\dagger(E', \vec{\Omega}' \rightarrow E, \vec{\Omega}). \quad (3.7)$$

In this case, the term 'adjoint' used to describe these new quantities has no mathematical derivation, it is simply an agreement to describe the transport properties of these new particles called adjunctons. Thus, by changing the direction of the reference system, it is possible to derive a transport equation for pseudoparticles

$$\begin{aligned} -\vec{\Omega} \cdot \nabla \phi^\dagger(\vec{r}, E, \vec{\Omega}) + \Sigma_t^\dagger(\vec{r}, E)\phi^\dagger(\vec{r}, E, \vec{\Omega}) &= S^\dagger(\vec{r}, E, \vec{\Omega}) \\ &+ \oint_{4\pi} d\vec{\Omega}' \int_0^\infty dE' \Sigma_t^\dagger(\vec{r}, E')f^\dagger(\vec{r}, E', \vec{\Omega}' \rightarrow E, \vec{\Omega})\phi^\dagger(\vec{r}, E', \vec{\Omega}'). \end{aligned} \quad (3.8)$$

The variable name replacement is used to emphasise that  $\psi(\vec{r}, E, \vec{\Omega})$  and  $\phi^\dagger(\vec{r}, E, \vec{\Omega})$  are not the same quantities, but are only distributed in the same way. Since a new type of particle is introduced, a new density function can be associated with it, and it can be shown that the equations (3.2) and (3.8) are formally identical and must respect the same boundary conditions [9], so the two solutions can overlap. Following the same steps as described above, it is still necessary to write the total collision kernel as a function of the partial collision kernels in such a way as to normalise them with respect to outgoing energy and directions.

$$f^\dagger(E', \vec{\Omega}' \rightarrow E, \vec{\Omega}) = \sum_{k=s,a,f} \frac{\Sigma_k^\dagger(E')}{\Sigma_t^\dagger(E')} \nu_k^\dagger(E') f_k^\dagger(E', \vec{\Omega}' \rightarrow E, \vec{\Omega}) \quad (3.9)$$

By substituting the two total kernel definitions, (3.5) and (3.9), within the equation (3.7), a relation can be found between them.

$$\sum_{k=s,a,f} \Sigma_k(E) \nu_k(E) f_k(E, \vec{\Omega} \rightarrow E', \vec{\Omega}') = \sum_{k=s,a,f} \Sigma_k^\dagger(E') \nu_k^\dagger(E') f_k^\dagger(E', \vec{\Omega}' \rightarrow E, \vec{\Omega}). \quad (3.10)$$

The model described by De Matteis [11] introduces two main assumptions: neutrons and adjunctons have the same set of reactions and the same collision rate. The second condition implies that the total cross sections for both particles have the same value

$$\Sigma_t(E) = \Sigma_t^\dagger(E) \quad (3.11)$$

meanwhile the first one allows to extend the relation imposed on the total collision kernels by the equation (3.10) to each pair of partial collision kernels:

$$\Sigma_k(E) \nu_k(E) f(E, \vec{\Omega} \rightarrow E', \vec{\Omega}') = \Sigma_k^\dagger(E') \nu_k^\dagger(E') f_k^\dagger(E', \vec{\Omega}' \rightarrow E, \vec{\Omega}). \quad (3.12)$$

These hypotheses are entirely arbitrary. Although the analogy between neutrons and adjoint cans seems natural and intuitive, it must be remembered that the only mathematical constraint comes from the adjoint relation between the two transport equations. Thus all possible alternative paths that satisfy the equation 3.7 are formally valid and equally viable.

Equivalence between partial sections can be introduced following the same idea

$$\Sigma_k(E) = \Sigma_k^\dagger(E). \quad (3.13)$$

Once the adjoint transport properties are defined, it is possible to compute all the partial collision kernels. The steps are made explicit in the paper by Saracco [12].

$$\nu_s^\dagger(E) = \frac{1}{\Sigma_s(E)} \oint_{4\pi} d\vec{\Omega} \int_0^\infty dE' \Sigma_s(E') f_s(E', \vec{\Omega} \rightarrow E, \vec{\Omega}'), \quad (3.14)$$

$$f_s^\dagger(E, \vec{\Omega} \rightarrow E', \vec{\Omega}') = \frac{\Sigma_s(E') f_s(E', \vec{\Omega}' \rightarrow E, \vec{\Omega})}{\oint_{4\pi} d\vec{\Omega}' \int_0^\infty dE' \Sigma_s(E') f_s(E', \vec{\Omega}' \rightarrow E, \vec{\Omega})}. \quad (3.15)$$

For the fission process yields

$$\nu_f^\dagger(E) = \frac{\chi(E)}{\Sigma_f(E)} \int_0^\infty dE' \nu_f(E') \Sigma_f(E'), \quad (3.16)$$

$$f_f^\dagger(E, \vec{\Omega} \rightarrow E', \vec{\Omega}') = \frac{\nu_f(E') \Sigma_f(E')}{4\pi \int_0^\infty dE' \nu_f(E') \Sigma_f(E')}. \quad (3.17)$$

In principle, it is only necessary to apply the normalisation condition for the outgoing energy and the angle of the adjoint collision kernel. The first novelty is the possibility of multiplying adjunctions also in the case of scattering: a possible misunderstanding could be the association between the path of a neutron and an adjunction, but the last consideration emphasises the distance between the two phenomena. The case of absorption is useless to present, since there are no particle distributions after the collision. The pseudo-fission properties are calculated by introducing the isotropic distribution with respect to the emission angle and the Watt distribution for the energy. It is important to note that in the case of isotropic emission it is possible to factorise the PDFs and sample each variable individually. The factor  $4\pi$  on the denominator is the scaling coefficient for the isotropic angle distribution. The Watt distribution is therefore a widely used approximation to the energy spectrum of neutrons emitted by fission.

### 3.3 Adjoint transport phenomena

Once a new type of particle has been introduced, it can be very useful to explore its physical properties. It must be clarified that the following thread will be purely speculative, as the adjunctions existence, i.e. the relations obtained, is limited within the simulation domain. Nevertheless, a clear insight into the differences between neutron and adjunction transport can become a powerful tool for taking advantage of reversed MC simulations.

The usual tendency is to observe the evolution of a particle's life and then derive a mathematical description capable of predicting the occurrence of each event. On the contrary, in this case it is necessary to start from the behaviour of PDFs and try to read all the clues to the definition of importance. Since the cross sections are the

same as for neutrons, the free flight sampling in the medium is unchanged. For the analysis of the scattering term, it may be useful to assume an isotropic scattering with an s-wave shape for the energy. This simplification can be made by taking into account that the phenomenon is not isotropic, but the cosine of the deflection angle depends on the ratio between the incoming and outgoing energy.

$$f_s(\vec{\Omega} \rightarrow \vec{\Omega}') = \frac{1}{4\pi}, \quad (3.18)$$

$$f_s(E \rightarrow E') = \frac{1}{(1-\alpha)E} \theta(E' - \alpha E) \theta(E - E'). \quad (3.19)$$

Where  $\alpha = \left(\frac{A-1}{A+1}\right)^2$ , with  $A$  the isotope mass number, and  $\theta(x)$  is the Heaviside unit step function. A simple substitution inside (3.14) and (3.15) yields

$$\nu_s^\dagger(E) = \frac{1}{(1-\alpha)\Sigma_s(E)} \int_E^{\frac{E}{\alpha}} dE' \frac{\Sigma_s(E')}{E'}, \quad (3.20)$$

$$f_s^\dagger(E \rightarrow E') = \frac{\Sigma_s(E') \theta(E - \alpha E') \theta(E' - E)}{E' \int_E^{\frac{E}{\alpha}} dE' \frac{\Sigma_s(E')}{E'}}. \quad (3.21)$$

The angular distribution is the same as for direct scattering. Looking at the equation (3.21) it is clear that the probability is strictly positive only for energies higher than the incoming one, so overall the adjunctons go from lower to higher energies. More interesting is the loss of normalisation of the outgoing scattering weight. The  $\nu_s(E)$  distribution is shown in the figure 3.1:  $U^{234}$ ,  $U^{235}$  and  $U^{238}$  are chosen as reference isotopes because most benchmarks are based on them. The data are taken from the ENDF-VIII library with a frequency of 200 values for decades. Since all functions are strictly greater than one, the adjoint can be multiplied without fissile material. Note that the integral part allows an analytical solution only for the cross section constant with energy:  $\nu_s^\dagger(E) = \frac{-\ln\alpha}{1-\alpha}$ , marked with a dotted line. The behaviour of the curves is quite constant: the effect is related to the high atomic number, which reduces the energy interval accessible to a particle. A better explanation is that the smaller the energy range of the integral, the more acceptable is the assumption of a constant cross section. This is confirmed by the fact that the peaks are in the resonance region. The integral must therefore be solved numerically, so the extremes impose a constraint on the detail of the nuclear data. The case of scattering with hydrogen is also worth mentioning because the integral is no longer upper bounded,

which leads to several difficulties in the encoding of both PDF and  $\nu_s^\dagger$ .

In order to analyse the fission term well, it must be remembered that the defi-

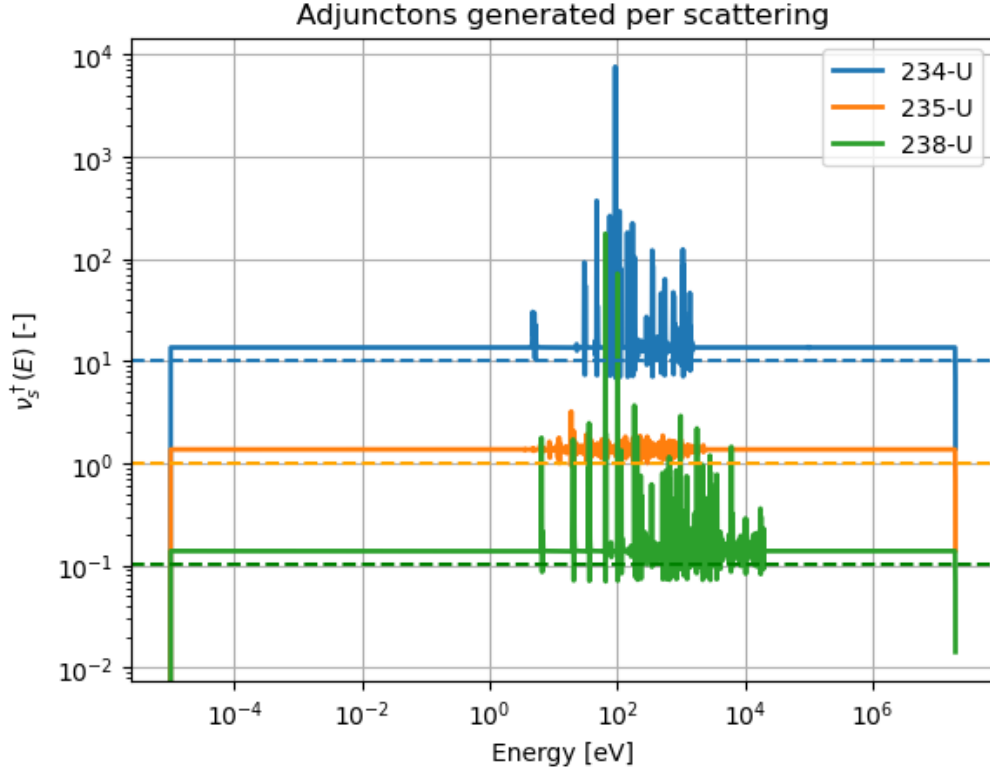


Figure 3.1: Adjunctons scattering multiplicity, value refers to  $U^{234}$  and  $U^{238}$  are increased and decreased by a factor of 10 respectively.

inition of importance for a critical system coincides with the probability of a neutron having a fission. It is therefore reasonable to assume that when a fission occurs in the neutron phase space, one or more adjunctons are produced. On the other hand, the number of adjunctons produced and their distribution is not straightforward. Equations (3.17) and (3.16) allow to construct graphs as a function of the outgoing energy: these are shown in figures 3.2 and 3.3 respectively. The cross-sectional data are taken from the ENDF-VIII library and are referenced to  $U^{235}$ , while the Watt distribution can be read in the Haghigat's book [14]. Looking at figure 3.2, it is easy to see the characteristic peak around  $1MeV$  of the fast neutrons. On the other hand, the spectrum of the adjunctons is widely distributed and dominated by the  $\Sigma_f(E)$  behaviour. Since the effect of the resonance region is not noticeable in the linear scale, it should be emphasised that the two curves are reported with different y-axis scales. Remembering the background information on the importance properties given in Section 3.1, it is clear here how the detector of the direct problem

acts as a source for the adjoint: adjunctons are emitted with an energy spectrum very similar to that of fission-causing neutrons. From the implementation point of view, this irregularity represents a considerable burden, since the energy has to be sampled by the rejection method, and the unresolved resonance region, which is characteristic of each isotope, drastically reduces the efficiency.

The other graph shows the adjunton multiplicities,  $\nu^\dagger(E)$ . Again, different scales are added to the curves: this allows the effect of the fission cross section to be better appreciated. For neutrons, the value is more or less constant with energy, except for a sharp change at very high energy, but the effect can still be considered negligible for no-fast applications. For pseudoparticles, the leading term is the Watt distribution: since the scale is log-log, the curve can be approximated by an exponential function. The most important aspect is the huge difference in the total number of particles produced, which can be explained by a mathematical formulation: Since the product  $\nu_f(E) \cdot f_f(E \rightarrow E')$  must be kept constant, the normalisation factor of the dagger PDF is reflected in  $\nu_f^\dagger(E)$ . On the other hand, the phenomenon is self-compensating, since low energy adjunctons are most likely to be emitted, while only high energy interactions can produce large numbers of particles. There is a clear correspondence in the direct neutron transport, since most of them are born in the fast region, but the probability of fission is higher if they are thermalised.

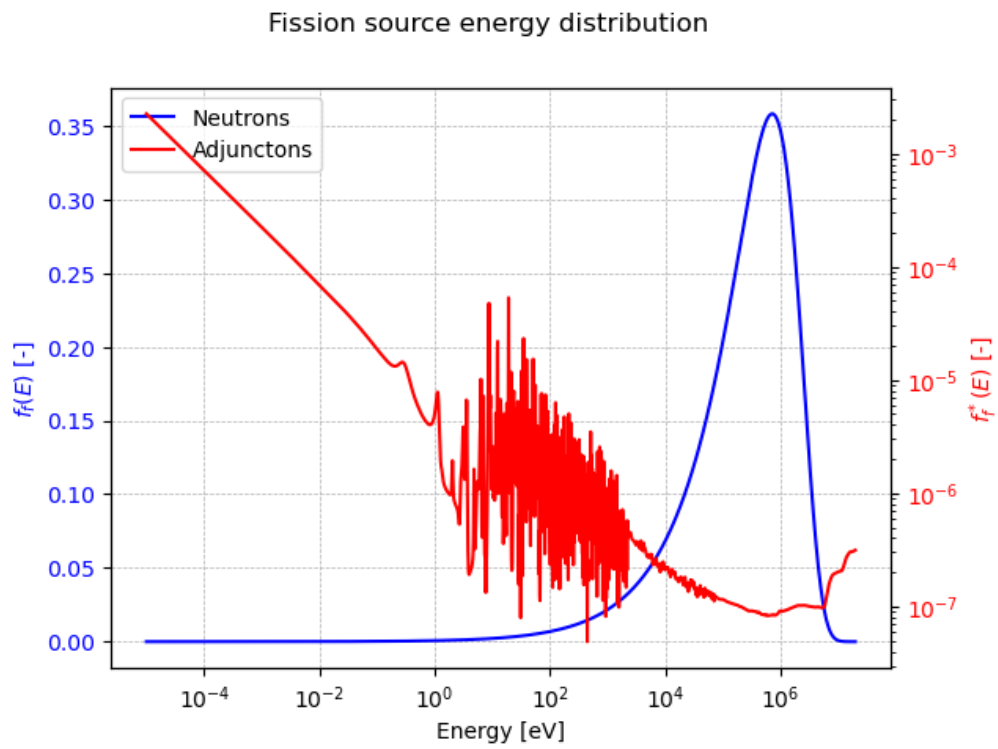


Figure 3.2: Neutron and adjunton energy emission spectrum

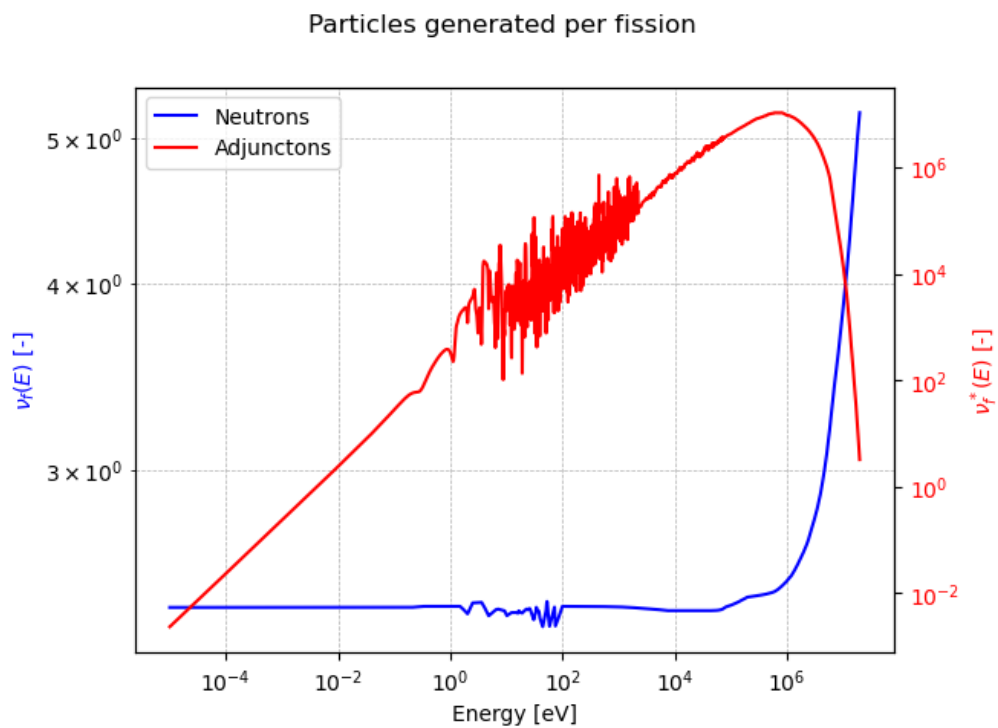


Figure 3.3: Neutron and adjunton number of particle emitted per fission

# Chapter 4

## An in-house Monte Carlo code

### 4.1 Generalities

All the results presented in this paper are obtained by an in-house MC code developed in Python. Its main feature is the ability to switch between direct and adjoint transport in a friendly way, using the model proposed in the Chapter 3. First, it is possible to implement it in commercial MC codes by changing only the nuclear inputs, as shown in the previous paragraphs. On the other hand, the main objective is to test the validity of the model. Therefore, the procedure indicated is not applied, in favour of the possibility to better detect errors or to identify points that require more careful treatment. In this way, a function is constructed for each transport process and, if necessary, additional lines are used to adapt the output depending on the particle being treated. Figure 4.1 shows graphically how the code is configured: each block represents a function, so blocks with the same name are the same functions, even if they are in different branches. The only missing information is that the check between eigenvalue problems and source-driven problems has to be done by the user when the simulation is configured.

The code is capable of representing infinite and homogeneous media or  $1D$  geometries such as spheres or plates. In both cases, it is possible to define a fixed source or to perform  $K$ -eigenvalue calculations. Random variables related to particles are sampled from continuous phase space: nuclear data as a function of incident particle energy are taken from the ENDF-VIII library with 200 values for each decade, intermediate cases are built by linear interpolation. To obtain sufficient resolution at all energy levels, the points are chosen to be logarithmically equidistant. Fur-

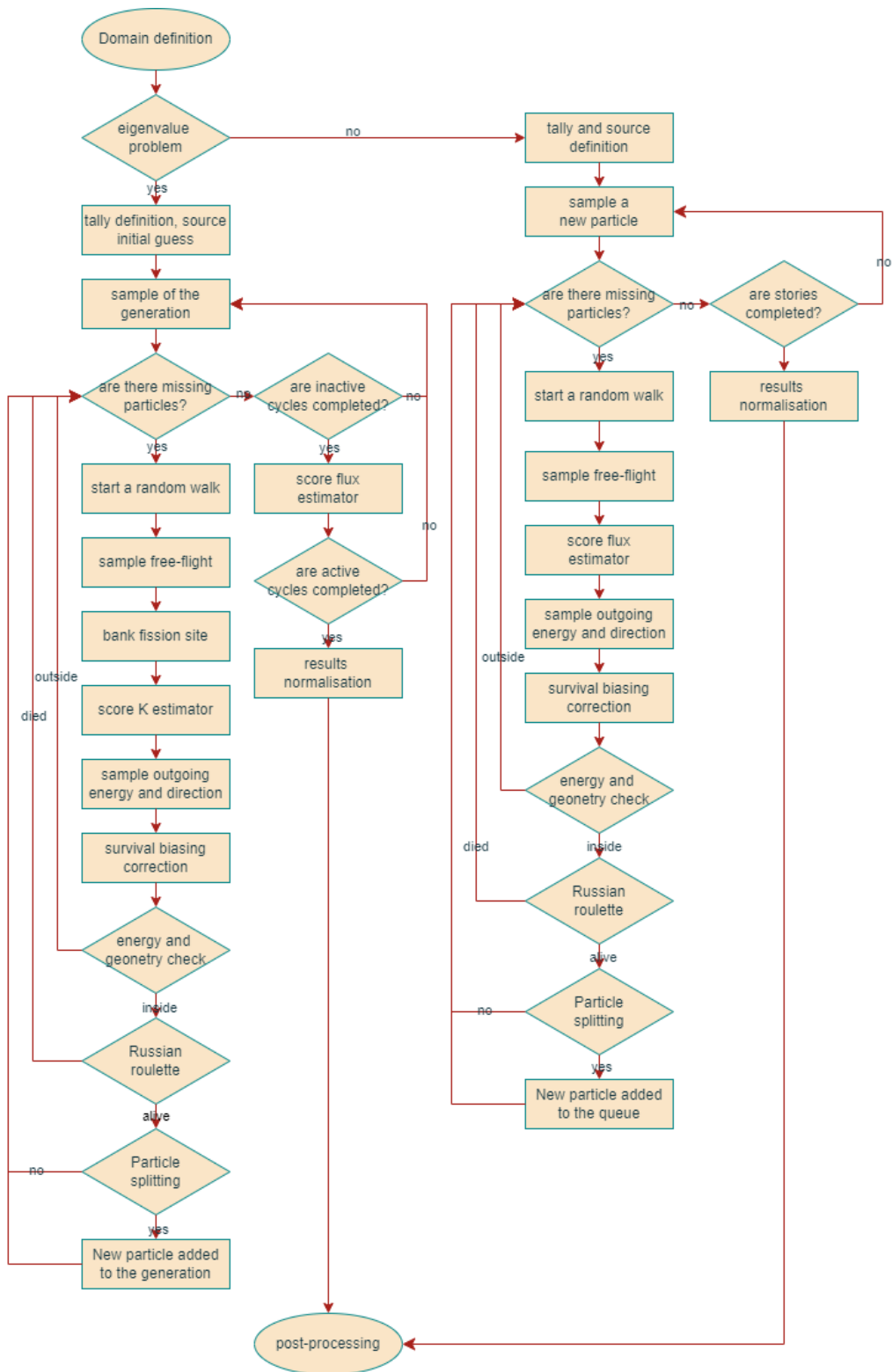


Figure 4.1: Monte Carlo code flow chart

thermore, the minimum and maximum energies are constrained to be  $10^{-5}$ eV and 20MeV respectively.

Non-analogue approaches are used to reduce the computational cost and increase the accuracy of the results. Survival bias, Russian roulette and particle splitting are the main VR techniques used, while in eigenvalue problems some bias is applied to limit the population increase or decrease.

## 4.2 Particle sampling

The particle object is defined as a mutable structure containing information about its state in phase space: position, energy and direction, completed by statistical weight and particle nature (i.e. neutron or adjunctor). To sample a new particle, each property must be treated independently to avoid bias introduced by possible correlations between random variables. In addition, all relevant data is grouped within the source structure.

Position sampling depends only on the nature of the problem to be solved. In source-driven systems, the spatial distribution of the source must be provided by the user as input. As the data format must be a vector of points, sampling is simply done by selecting a random index. If not specified, the default is to start at the axis origin. In the eigenvalue case, however, an iterative process is required to build up an affordable source space distribution. The initial guess can be specified in the same way as before, or by default is at the axis origin. Again, the fission site points are collected into vectors as a function of the principal direction (i.e. in spherical geometry the principal direction is the radius), but no sampling is required between them since all sites will produce at least one particle.

The flight direction is sampled by a uniform PDF on the spherical surface.

$$\varphi = 2\pi\eta_1, \tag{4.1}$$

$$\theta = \sin^{-1}(2\eta_2 - 1), \tag{4.2}$$

where  $\eta$  is a random number uniformly distributed between 0 and 1. It is important to note that since the random number to be generated must be independent, both  $\eta$  values must be sampled separately. This approach is representative of all directional sampling in the code, since the isotropic condition is always true.

The energy sampling is the most complex and, as mentioned above, represents a crucial difference between the direct and adjoint simulations. It is possible to define the source in three different main categories: 'mono-energetic', 'fission' and 'custom'. The former require that the initial energy of the particle is always equal to the specified value, an application that will be considered later in the discussion of the slowing down problem. The 'fission' mode includes all the procedures developed to reproduce well the fission emission spectrum. For neutrons, the energies are taken from the Watt spectrum according to the procedure proposed by Haghghat[14].

$$i) \quad k = 1 + \frac{b}{8a}$$

$$ii) \quad L = a^{-1}(k + \sqrt{k^2 - 1})$$

$$iii) \quad x = -\ln(\eta_1), \quad y = -\ln(\eta_2)$$

$$iv) \quad M = aL - 1$$

$$v) \quad \text{If } y - M(x + 1)^2 \leq bLx, \text{ return } E' = Lx.$$

While  $a$  and  $b$  are tabulated constants that are different for each isotope, the same values are often used in general Watt spectra. Although it may not seem so clear, the general idea is to use a standard rejection method, but the shape of the auxiliary function is optimised to increase efficiency. The need for this additional focus on sampling efficiency becomes very clear when recalling Figure 3.2: the standard rejection method uses a rectangle for linear sampling and only accepts points inside the blue curve, so the presence of the peak imposes a huge increase in the area subtended. Note that the efficiency of the rejection method can be calculated as the ratio between the integral of the PDF to be reproduced and the integral of the auxiliary function. This digression is fundamental to understand the relevance of the proposed procedure for the sampling of the energy distribution of the adjunctons. Returning to Fig. 3.2, it is necessary to implement a method capable of reproducing the red curve. The simplest and most intuitive solution is to use the standard rejection method. Given  $E_0 = 1 \cdot 10^{-5}$ eV and  $E_1 = 20$ MeV

- i)  $E' = E_0 + (E_1 - E_0)\eta_1$
- ii)  $M = \max(f_f^\dagger(E))$
- iii) if  $\eta_2 M \leq f_f^\dagger(E')$  return  $E'$ .

The graphical representation is shown in figure 4.2. Several attempts underline the extreme computational time needed to sample an adequate number of random numbers. As a benchmark, a simple calculation can be performed to evaluate the efficiency of the procedure: all values are related to  $U^{235}$ . The maximum point is around  $y_{max} = 5 \cdot 10^{-4}$ , so the area inside the rectangle is  $A = 10^4$ . Since the emission spectrum is normalised, the efficiency is  $\epsilon_{std} = 10^{-4}$ : on average, for each output to be produced, it is necessary to generate  $10^4$  pairs of random numbers,  $\eta_1$  and  $\eta_2$ . Therefore, this work proposes an alternative procedure that aims to significantly reduce the computational effort and time.

It is called logarithmic rejection and is based on modifying the auxiliary function to follow the behaviour of the energy PDF. Roughly, you want to increase the frequency of low values and vice versa. So, as the name suggests, a logarithmic distribution is used as the auxiliary function for the rejection method.

$$g(E) = \frac{M}{E(\ln E_1 - \ln E_0)}, \quad (4.3)$$

where  $M$  is an arbitrary value chosen so that the auxiliary function is always above the PDF to be sampled. The shape of this curve is shown in the figure 4.2. Starting from the calculation of the factor  $M$ , the simplest choice would be to select it by comparing  $\min(g(E))$  with  $\max(f_s^\dagger(E))$  according to the standard rejection method. However, this solution runs the risk of being self-defeating: since the area covered by the logarithmic curve will always be larger than in the standard case, this can be easily demonstrated by imagining that in figure 4.2 the orange curve is shifted upwards. In this case, the value of  $M$  is computed iteratively: given an initial guess, it is tested whether the majority condition is satisfied for all points, and otherwise the value is increased. For the following calculations,  $M = 55$  is used. Note that although in general different isotopes require different values of  $M$  to construct an optimised function, in this case it is the same with an accuracy of the first integer digit.

Returning to the reasons for choosing the auxiliary function,  $g(E)$  is also useful because it allows the application of the inverse transform method for sampling the random variable, the implementation of which is reported below. Thus, although some ad hoc functions can be constructed to better approximate the shape of the adjoint fission spectrum, the candidate is still recommended because the sampling of the random variable is straightforward: only a linear sampling of the exponent needs to be performed.

$$E' = 10^{\log_{10} E_0 + (\log_{10} E_1 - \log_{10} E_0)\eta}. \quad (4.4)$$

Finally, the acceptance probability must be rearranged to the new auxiliary function. The condition to fulfil is

$$\frac{f_f^\dagger(E)}{g(E)} \leq 1 \quad \forall E. \quad (4.5)$$

Hence the probability of accepting the proposed value,  $E'$ , is

$$\eta \leq \frac{f_f^\dagger(E')}{g(E')} = f_f^\dagger(E') \cdot \frac{E'(\ln \frac{E_1}{E_0})}{M}, \quad (4.6)$$

where  $\eta$  is always a random number uniformly distributed between 0 and 1. It is interesting to note how the transition from a linear space, standard rejection, to a logarithmic space, logarithmic rejection, leads to a self-correction of the statistic. The term  $E'$ , which is used within the equation (4.3) to increase the frequency of low energies, acts within the equation (4.6) to facilitate the selection of higher energies. To simplify the implementation, it is possible to collapse the term  $\frac{M}{\ln \frac{E_1}{E_0}}$  into a single constant, but the extended notation is preferred to make the domain of the function explicit.

Once the robustness of the procedure has been proven, the implementation steps are resumed.

$$i) \quad E' = 10^{\log_{10} E_0 + (\log_{10} E_1 - \log_{10} E_0)\eta_1}$$

$$ii) \quad L = f_f^\dagger(E') \cdot E'(\ln \frac{E_1}{E_0})$$

$$iii) \quad \text{if } \eta_2 M \leq L \text{ return } E'.$$

Figure 4.3 shows the result of a series of tests aimed at estimating the effective gain in computation time due to the logarithmic rejection implementation. The

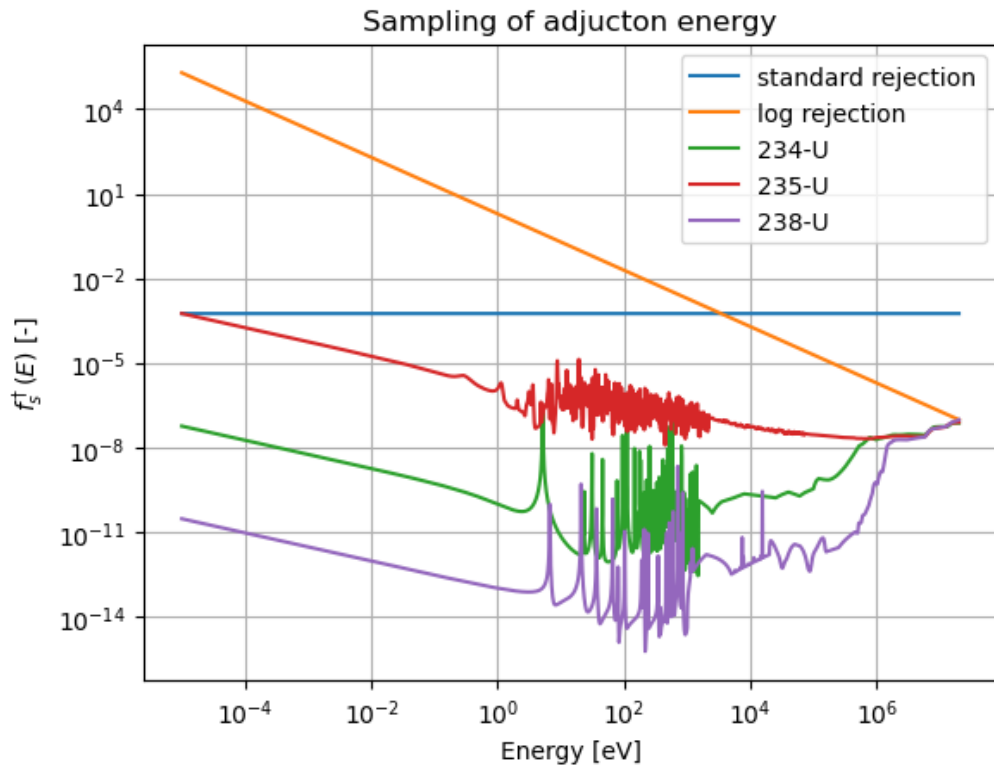


Figure 4.2: Comparison between adjoint fission spectrum and sampling functions

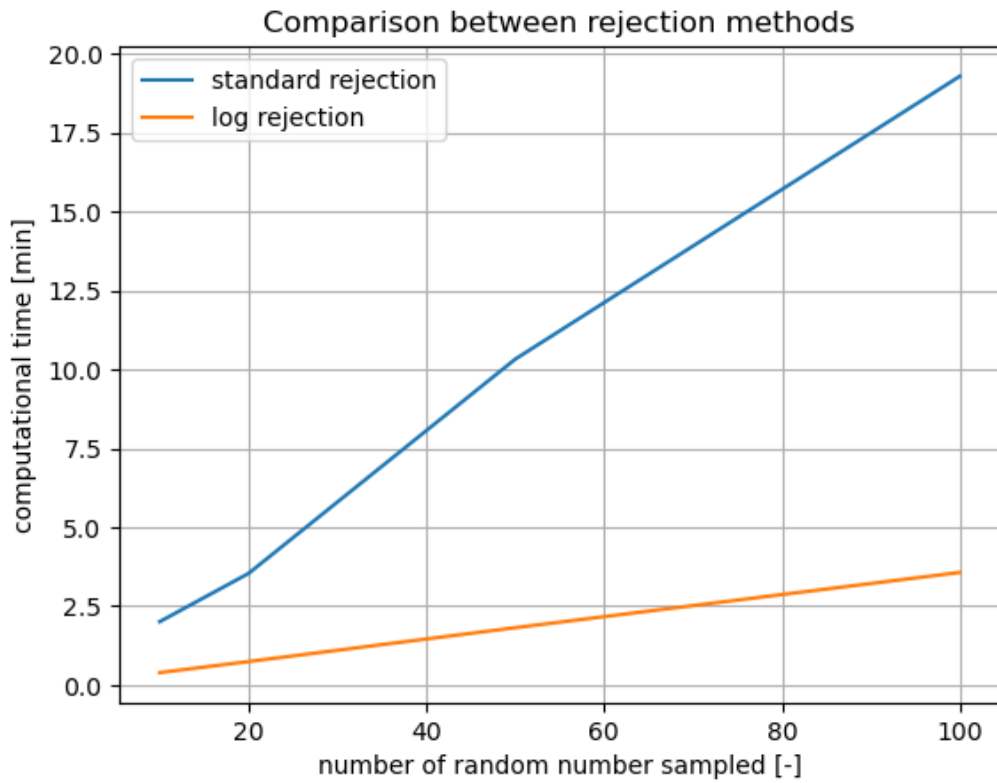


Figure 4.3: Comparison between rejection methods performance

curves are extrapolated from four measurements where 10, 20, 50 and 100 random numbers had to be provided. The behaviour is almost linear in all cases, indicating the constant efficiency of the rejection method. To give an idea of the improvement, a good 'rule of thumb' for selecting the number of particles to simulate in each cycle for the power iteration method suggests at least 200 particles per tally. Considering the linear trend of the curves to be affordable, the standard rejection method will spend around 40min for each tally just to sample the initial energy distribution. Meanwhile, the proposed alternative is capable of performing the same task in less than 10min. For completeness, the theoretical efficiency of the logarithmic rejection method is also given.

$$\epsilon_{log} = \frac{\int_{E_0}^{E_1} dE f_f^\dagger(E)}{\int_{E_0}^{E_1} dE g(E)} = \frac{1}{M} = \frac{1}{55}. \quad (4.7)$$

So  $\epsilon_{log} \gg \epsilon_{std} = 10^{-6}$ . The empirical results can be confirmed by looking at the figure 4.2: although the area under the orange curve appears larger than the area under the blue curve, the right side of the graph has a drastically higher weight due to the logarithmic scale. The improvement in efficiency,  $\frac{\epsilon_{log}}{\epsilon_{std}}$ , is larger than the effective improvement in computation time,  $\frac{t_{log}(N)}{t_{std}(N)}$ , because an important contribution comes from standard machine operations. These are neglected because they are not the objective of this work.

The logarithmic rejection method can also be a useful tool for sampling cross section values. Recalling the definition of  $f_f^\dagger(E)$  and identifying the fission cross sections as the dominant term, the suitability of the procedure for the new task is self-evident.

### 4.3 Free flight sampling

The interaction between particles and matter is an inherently random phenomenon: the cross section is physically defined as the probability per unit path that the particle will have an interaction. So the probability of an interaction occurring in a

small interval can be written as

$$P_1(r) = \Sigma_t(r, E)dr. \quad (4.8)$$

Meanwhile, to have a complete description of the probability of interaction around a chosen point, it is also necessary to consider the probability of the particle travelling to position  $r$  without interacting

$$P_2(r) = e^{-\int_{r_0}^r dr' \Sigma_t(r', E)}. \quad (4.9)$$

where  $r_0$  is the initial position and the notation  $r$  is always used to refer to  $|\vec{r}|$ . Since both events must occur and they are independent, it is sufficient to multiply them, and the general form of the equation (3.4) is derived.

$$p(r)dr = \Sigma_t(r, E)e^{-\int_{r_0}^r dr' \Sigma_t(r', E)} dr \quad (4.10)$$

Note that  $P_1(r)$  and  $P_2(r)$  are probabilities, whereas  $p(r)$  is a probability density function, so the infinitesimal motion must be counted. In accordance with dimensional analysis, the unit of measure for  $p(x)$  is the same as  $\Sigma_t(r, E)$ . Another important detail is the loss of energy dependence between the two sides of the equation: since the particles do not interact until the collision occurs, their energy is constant, so the cross sections depend only on position. The equation (3.4) represents the case where the path is only within a single material. Only in this case is it possible to solve the integral analytically, so the inverse transform method is used to sample the path length.

$$l = -\frac{\ln(\eta)}{\Sigma_t(r_i, E)} \quad (4.11)$$

where  $r_i$  does not describe the exact position of the particle, but only the medium. On the other hand, the potential applications of this method are rather limited, since only experimental reactors are usually made of a single homogeneous material. A possible solution for systems made of layers of homogeneous materials may be to sample a free flight and, if the particle crosses the boundary between two materials, to repeat the sampling. This approach is a common choice for MC codes, but requires the generation of multiple random numbers, especially for highly layered geometries. With the aim of testing an implementation of an optimised solution,

it is preferable to adopt the alternative solution proposed by Haghghat [14]. The choice is justified by the fact that it involves the generation of a single random number, which is often the most expensive task for a computer. The general idea is to rewrite the equation (4.10) in terms of the mean free path (mfp) and use it as the unit of distance. The mfp is defined as the expected distance a particle will travel undisturbed.

$$\lambda = E[r] = \int_0^R dr \Sigma_t(r, E) e^{-\Sigma_t(r, E)r}. \quad (4.12)$$

This is just the definition of the first order moment for a random variable. For a homogeneous material the calculation is very simple:  $\lambda = \frac{1}{\Sigma_t(r_i, E)}$ . This definition can be applied to the equation (4.11).

$$l = -\frac{\ln(\eta)}{\frac{1}{\lambda}}. \quad (4.13)$$

In this way a new random variable can be defined as follows

$$b = \frac{l}{\lambda} = -\ln(\eta). \quad (4.14)$$

In order to provide the reader with as detailed a description as possible, the steps to implement this algorithm in a sphere with homogeneous layers will be explained. Let  $r_0$  be the particle position and  $d_i$  the distance between the particle position and the surface to be crossed to overcome the relative layer.

- i)* Identify the direction of flight (i.e. outwards from the centre);
- ii)* construct a vector  $\bar{r}$  such that  $r[0] = d_1$  and  $r[i] = d_i - d_{i-1}$  for  $i > 0$ , the enumeration must follow the order in which the particle will encounter the materials;
- iii)* construct the vector  $b$  as  $b[i] = \sum_{j=0}^i r_j \Sigma_t(r_j, E)$ ;
- iv)* sample  $b = -\ln(\eta)$ ;
- v)* for each material, enumerate as  $m$ , define  $b_{m-1} = b[m-1]$  if  $m > 1$  else  $b_{m-1} = 0$  and  $b_m = b[m]$ ;
- vi)* stop the cycle when it finds  $m$  such that  $b_{m-1} < b \leq b_m$ ;
- vii)* calculate  $l = \frac{b - b_{m-1}}{\Sigma_t(r_m, E)}$ ;

*viii)* move the particle along the direction of flight for  $L = l + r[m - 1]$ .

The notation is consistent with Python's vector enumeration, so it should be adapted depending on the programming language (i.e. in Python, access to the first element is done using 0 as index). Special care must be taken when flying towards the centre of the sphere: first, the list of sub-regions must be read in reverse to follow the particle's path, and finally, once the list has ended at the inner material, the same scheme must be applied to follow the particle's path outwards. The reason for this can be understood by trying to imagine a hypothetical path of the particle: if it is able to reach the inner part, it will be projected onto the opposite part of the sphere, so that the relationship between the direction of flight and the vector normal to the sphere's surface is reversed. Obviously, all the indices must also be rearranged to match the order imposed by the displacement.

In order to verify the performance of the proposed procedure in the treatment of interfaces, a series of experiments are carried out. The domain can be described as an ideal sphere,  $R = 10\text{cm}$ , consisting of a single block of pure  $C^{14}$ . It is divided into 99 equally spaced tallies. The idea is to introduce two dummy interfaces along the radius to simulate the presence of different layers, but without changing the material: the aim is to isolate any possible error related only to the numerical models implemented. It is therefore expected to be able to reproduce the results obtained in the simplified case. The setup involves the introduction of  $10^5$  particles, all emitted at the same energy 1MeV and position,  $\vec{r}_0 = (0, 0, 0)$ . Figures 4.4 and 4.5 compare the neutron flux shape, with a  $\pm 3\sigma$  confidence interval, before and after domain partitioning; grey lines are used for clarity only. The results can be considered successful, as the introduced variation is very small with respect to the flux value: note that the vertical axis is on a logarithmic scale, so small values are emphasised. Nevertheless, the number of tallies used is deliberately exaggerated in order to highlight even the smallest discontinuities. Finally, it is important to note that the slope of the curve is unchanged. The same conclusions can be drawn from the solution of the adjoint problem, figures 4.6 and 4.7. In this case, the continuity of the curve is even better than in previous calculations, while the code is exactly the same. The difference is due to random numerical fluctuations inherent in MC applications.

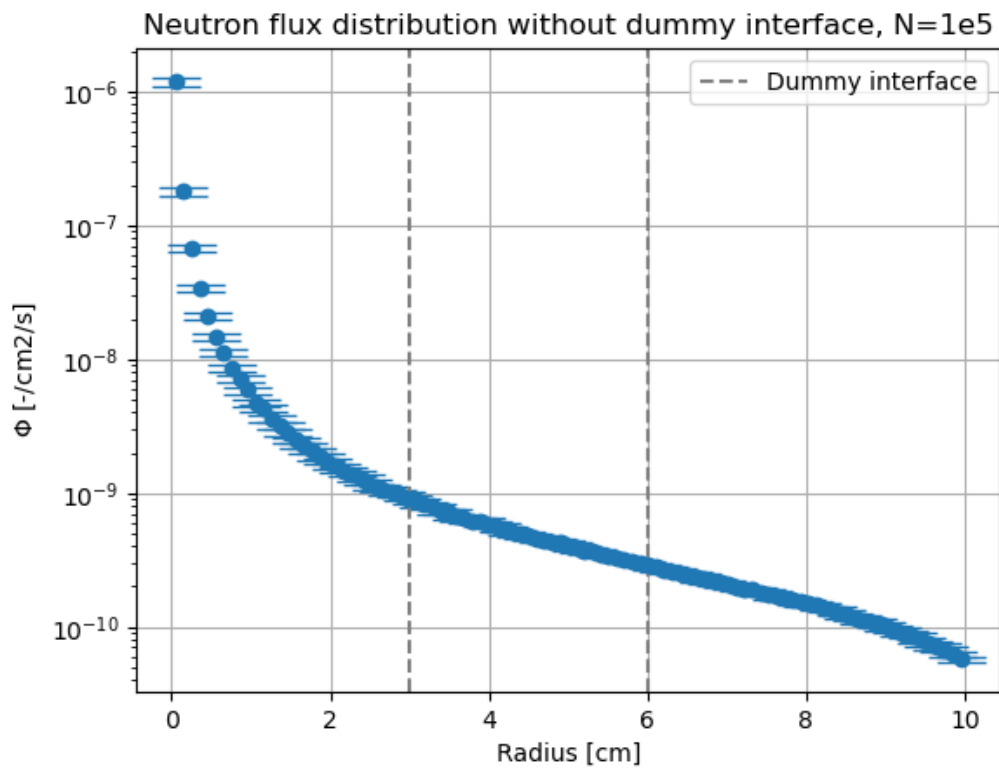


Figure 4.4: Test on interface treatment, Neutrons

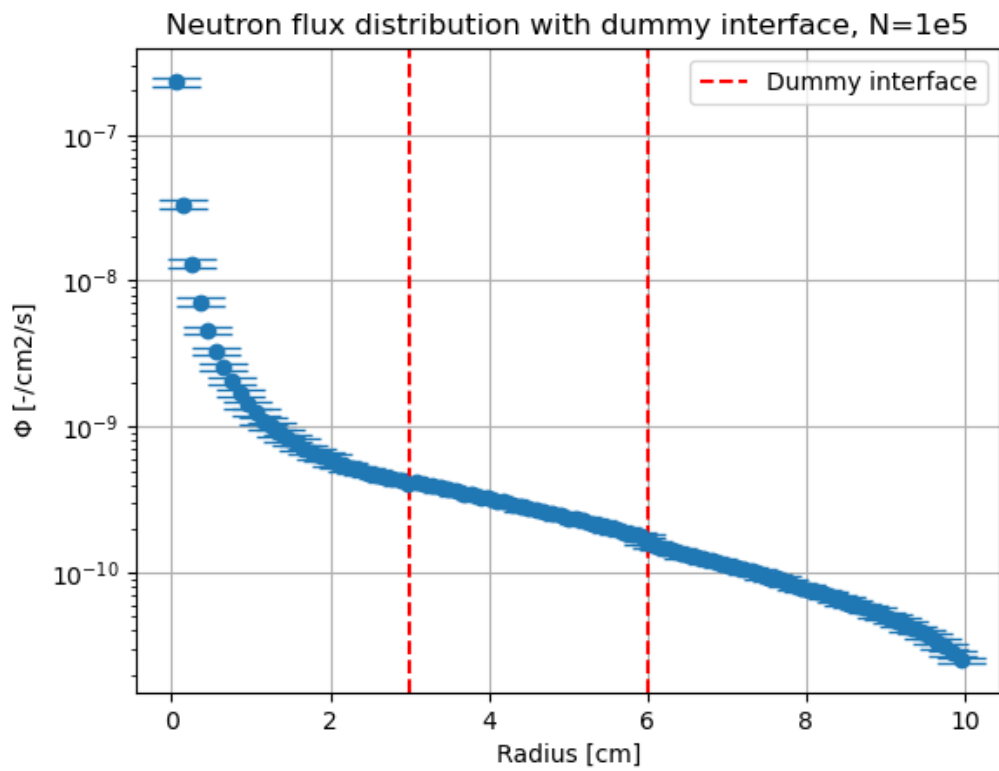


Figure 4.5: Test on interface treatment, Neutrons

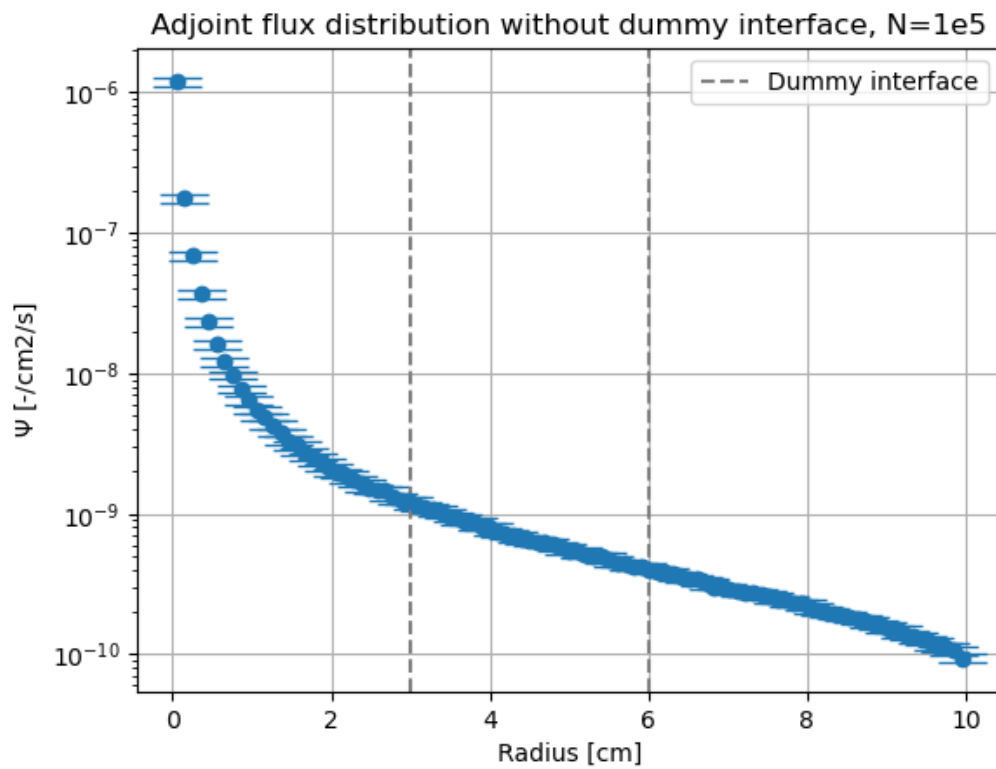


Figure 4.6: Test on interface treatment, Adjunctons

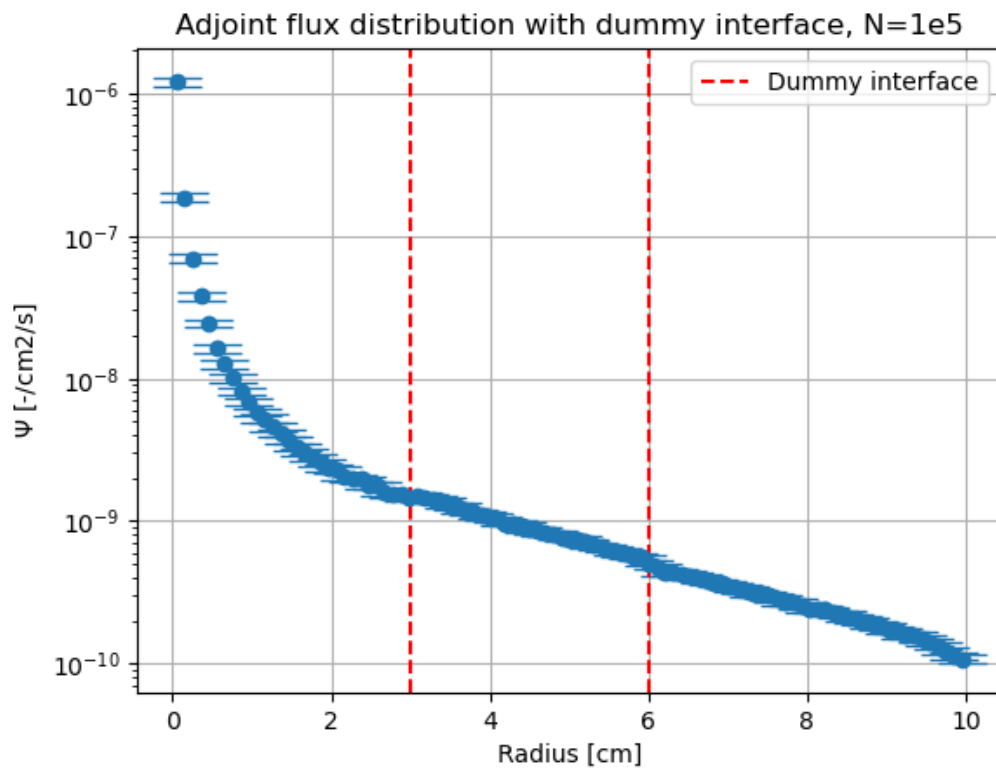


Figure 4.7: Test on interface treatment, Adjunctons

## 4.4 Energy sampling

Taking into account the lifetime of the particle, its properties must be updated once the interaction has occurred. As mentioned above, the only scattering phenomena modelled are the elastic and isotropic cases. Isotropism imposes that each direction of flight is equally likely, while the elastic approximation allows the use of the Heaviside unit step function. The PDF governing the phenomenon is represented by the Equations (3.18) and (3.19).

$$f_s(\vec{\Omega} \rightarrow \vec{\Omega}') = \frac{1}{4\pi},$$

$$f_s(E \rightarrow E') = \frac{1}{(1-\alpha)E} \theta(E' - \alpha E) \theta(E - E').$$

As mentioned above, the angle distribution is the same for neutrons and adjunctons, while the sampling procedure can be founded in the Equations (4.1) and (4.2). Regarding the treatment of the energy variable it is important to note that  $f_s(E \rightarrow E')$  can be integrated, so sampling can be performed by inverse transform method. Remembering that the variable to sample is  $E'$ :

$$F_s(E') = \int_0^{E'} dE'' f_s(E \rightarrow E'') = \frac{1}{(1-\alpha)E} \int_0^{E'} dE'' \theta(E'' - \alpha E) \theta(E - E'').$$

The solution of the integral is straightforward

$$\eta = \frac{1}{(1-\alpha)E} (E' - \alpha E),$$

$$E' = \alpha E + (1-\alpha)E\eta. \quad (4.15)$$

So the possible outgoing energies of the neutrons are bounded between  $E$  and  $\alpha E$ , note that  $\alpha < 1$ , and the Equation (4.15) is nothing but a linear sampling between them.

On the other hand, a more structured and complex process is required for managing post-collision energy of adjunctons. It may be useful to have a look at the Equation (3.15)

$$f_s^\dagger(E \rightarrow E') = \frac{\Sigma_s(E') \theta(E - \alpha E') \theta(E' - E)}{E' \int_E^{\frac{E}{\alpha}} dE' \frac{\Sigma_s(E')}{E'}}.$$

The main difficulty came from the extremes of the integral in the denominator: unlike fission, the interval range depends on the incoming energy, making the construction of a function much more challenging. The implemented algorithm therefore includes its calculation for each collision. Contrary to the previous guideline, in this case the simpler solution is preferred to the optimised one for two main reasons: the implementation and debugging processes are much easier, while the computational cost introduced is less relevant. The steps are as follows.

- i)*  $\alpha = \left(\frac{A-1}{A+1}\right)^2$ ;
- ii)* find the last  $E_l < E$  in the energy vector;
- iii)* find the first  $E_u \geq E$  in the energy vector;
- iv)* define the vector  $\overline{E} = [E_l, \dots, E_u]$ ;
- v)* define the vector  $\overline{\Sigma} = [\Sigma_s[E_l], \dots, \Sigma_s[E_u]]$ ;
- vi)* compute  $\mathcal{S} = \int_E^{\frac{E}{\alpha}} dE' \frac{\Sigma_s(E')}{E'}$  numerically;
- vii)* define  $f(E') = \frac{\Sigma_s(E')}{E'} \cdot \frac{1}{\mathcal{S}}$ ;
- viii)* apply standard rejection method on  $f(\overline{E})$ .

The notation may seem forced, but it is necessary to distinguish the coding domain from the mathematical domain. Even if the code is based on a continuous energy model, the implementation imposes the definition of a vector of energies coupled to the vector of cross sections to be imported. Thus  $E_l$  and  $E_u$  represent the values or their indices stored in the elements of the energy vector. So  $\overline{E}$  is a collection of elements extrapolated from the energy vector. Following the same reasoning,  $\Sigma_s[E]$  is the value collected within the cross section vector corresponding to the specified energy value. Here, the standard cross section method is chosen over the logarithmic version presented in the previous section because, since the domain extension is quite small, the efficiency value is definitely higher. The slowing down case study discussed in Chapter 5 can also be read as a verification of this sampling procedure.

## 4.5 Variance reduction techniques

Non-analog MC codes are characterised by the application of some 'corrections' to the PDFs in order to favour more useful results. To recall the case of the shielding problem, the high probability of capture prevents particles from reaching the detector, thus reducing the number of histories that are useful for estimating the particle flux over the edge. It is therefore possible to increase the probability of the particle surviving without changing the average result. The book by Haghigat[14] reports the basic constraint to be met.

$$w_{unbiased} \cdot f_{unbiased} = w_{biased} \cdot f_{biased}. \quad (4.16)$$

This equation introduces a new property associated with the particle called the statistical weight. It is a correction factor applied to preserve the expected physical result during the transition from the original to the biased PDF.

Survival bias is a widely used VR technique based on imposing a scatter probability equal to one. Since the scatter probability for a particle is  $p_s = \frac{\Sigma_s}{\Sigma_{tot}}$ , from the equation (4.16),  $w_{biased} = w_{unbiased} \cdot \frac{\Sigma_s}{\Sigma_t}$  can be easily calculated. A more common way of presenting the result is  $w_{biased} = w_{unbiased} \cdot (1 - \frac{\Sigma_a}{\Sigma_t})$ . So each time the particle is forced to survive, its contribution to the score is reduced by a factor equal to the effective probability of survival. This trick makes it possible to increase the number of significant events in regions relatively far away from the source, but on the other hand it may happen that particles with very low weight continue to be simulated. In other words, since a cause for the end of a random walk is neglected it is necessary to introduce a way to kill meaningless simulations.

Russian roulette is a stochastic method designed to handle low weight particles without distorting the averaged results. Starting from the choice of a cut-off for the minimum particle weight, it is compared to a random variable uniformly distributed between one and zero,  $\rho$ . The weight of the particle can be interpreted as the probability of surviving the game: if  $\rho \leq w$ , the particle weight is set to one, otherwise the random walk is term.

Building on the idea of using a particle's weight as a measure of its statistical

contribution, the introduction of an upper limit becomes essential to mitigate large fluctuations. This approach, known as particle splitting, involves splitting the original particles into smaller "daughters" while preserving the overall weight. Thus, once  $w \geq w_{max}$ :

- if  $n = \frac{w}{w_{max}}$  is an integer, as many identical new particles will be created with  $w' = \frac{w}{n}$ ,
- if  $n = \frac{w}{w_{max}}$  is real, a random sampling between  $INT[n]$  and  $INT[n] + 1$  must be performed with  $p_{INT[n]+1} = n - INT[n]$ , so the new weight is adjusted depending on the number of outgoing particles.

It is important to clarify that the operator  $INT[-]$  does not refer to the standard mathematical rounding procedure, but to the specific integer truncation function used in the calculation. The coupling between Russian roulette and particle splitting is often presented as a weight window technique, since the particle weight domain is reduced to a closed interval. The same approach can be applied using any parameter other than particle weight as a benchmark: a common case is to divide the domain into sub-regions and assign them different levels of importance,  $I$ . The procedure presented is the same, but it is necessary to adapt the trigger conditions so that Russian roulette is applied when  $I_1 < I_0$  and particle splitting when  $I_1 > I_0$ , with  $n = \frac{I_1}{I_0}$ . Where the random walk goes from  $I_0$  to  $I_1$ .

## 4.6 Population control techniques

Moving from general cases to eigenvalue calculations, a bias is commonly introduced into fission's site sampling in order to limit population growth or decline. It may be useful to give an example of the problem associated with non-critical systems solved by the power method. Given an initial population,  $N_0$ , and recalling the definition of the first eigenvalue,  $K$ , the population at a generic cycle,  $n$ , can be simply expressed as

$$N_n = K^n \cdot N_0. \quad (4.17)$$

Thus, considering  $K = 1.2$  at the 30<sup>th</sup> cycle, the population will be more than 200 times higher, whereas in a subcritical system all neutrons will be extinguished. Population control techniques are a large family of methods developed to keep the

number of simulated particles more or less constant at each cycle.

The expected number of particles produced by a collision in a multiplicative medium can be written as  $R_i = w \cdot \frac{\nu \Sigma_f}{\Sigma_t}$ , where  $i$  is the single event. Simultaneously, this value can be used as an estimator of  $K_{eff}$ , it's presented in Haghghat's book as the collision estimator [14]. So one of the most common procedures is to use the actual value of  $K_{eff}$  as a bias for sampling the number of fission sites.

$$R_i = w \cdot \frac{\nu \Sigma_f}{\Sigma_t} \cdot \frac{1}{K_n} \quad (4.18)$$

To satisfy the condition imposed by (4.16), the statistical weight of the new particles must be equal to  $K_n$ . If  $R$  is a real number, sampling must be performed between the closest integers, as presented in the last section. An important aspect related to the bias PDF is that the total statistical weight of the generation is preserved: let's consider a supercritical system, the correction applied to the equation (4.18) will reduce the number of particles to be simulated while increasing their statistical weight,  $K_n > 1$ .

Another possible solution starts from the equation (4.17) and applies a normalisation procedure at the beginning of each cycle. Since the single cycle estimate of  $K_{eff}$  depends only on the ratio between the populations and not on their absolute value, it is possible to reduce or increase the total statistical weight of each generation in order to keep it constant,  $N_0$ . There are two possible treatments:

- **Russian roulette and particle splitting:** these techniques can be used to sample the desired number of particles from the original population;
- **Weight normalisation:** the particle weight is adjusted depending on the number of fission sites in the bank.

Since neither procedure is an application of bias to the PDF, conservation of total statistical weight is not required: it decreases for  $K > 1$  and vice versa. Note that in the first case, the number of particles in the fission bank is constant and they have an initial weight equal to one, imposed by Russian roulette and particle splitting. On the other hand, the normalisation keeps the weight equal for all particles, but the value can be different from one depending on  $K_n$ . In this case, the number of random walks to be simulated can also change.

## 4.7 Scoring

The final part of the code implementation discussion is devoted to data acquisition and the post-processing required to extrapolate coherent results. Theoretically, it is necessary to define a detector for the quantity of interest and derive its sensitivity to triggers. The most conventional approach is to simply count the number of particles interacting within a volume of phase space. This technique is called collision estimation: the space  $\vec{r}$  and energy  $E$  domains are discretised into  $N$  and  $M$  intervals, respectively, and then all particles that have had a collision within  $\delta r_n$  and  $\delta E_m$  are scored. Formally the detector response can be expressed as:

$$R(n, m) = R(n, m) + w. \quad (4.19)$$

In this case, the dependence on direction is neglected, although the same treatment can be applied to it. However, this simplification is common in most practical simulations, since integral quantities such as collision density and scalar flux are the main targets of interest, and the effort associated with handling angle-dependent quantities is trivial. It should be emphasised that in analogue MC simulations the value of  $w$  is always unitary. In order to pass from the number of particles to the collision density, it is necessary to normalise the value with respect to the dimension of the phase volume.

$$F(\vec{r}_n, E_m) = \frac{R(n, m)}{H \Delta V_n \Delta E_m} \quad (4.20)$$

where  $H$  is the total number of particles simulated,  $\Delta V_n$  is the volume of the detector and  $\Delta E_m$  is the energy range. To better explain how these intervals need to be calculated, let us consider the simplest possible case: 1D phase space. If a discretisation is applied to produce a vector of 100 elements,  $\bar{x}$ , this will represent the collection of boundary values between tallies. Thus  $x_n$  describes the centre of the tally. Following this model, the interval  $\Delta x_n$  must be evaluated as the difference between the original values. To obtain the scalar flux, it is necessary to recall the definition of the collision density:

$$F(\vec{r}, E) = \Sigma_t(\vec{r}, E) \phi(\vec{r}, E). \quad (4.21)$$

Hence the direct application resulted in

$$\phi(\vec{r}_n, E_m) = \frac{F(\vec{r}_n, E_m)}{\Sigma_t(\vec{r}_n, E_m)}. \quad (4.22)$$

On the other hand, as seen earlier, the cross sections can vary very significantly with energy, so choosing a single reference cross section to describe the whole small group can lead to erroneous results. The problem can be overcome by defining a new counter:

$$R'(n, m) = R(n, m) + \frac{w}{\Sigma_t(\vec{r}, E)}. \quad (4.23)$$

In this way it is possible to trace back to the original particle properties and avoid introducing any approximations. Depending on the objectives of the simulation, it is therefore necessary to choose the most efficient estimator. The book by Haghghat [14] presents a number of alternative solutions and the criteria to choose depending on the properties of the medium. The collision estimator is the only one that has been implemented in the present work.

Looking at the global scheme of an MC code, the effective role of the estimator is nothing more than the random variable to be sampled. In order to better explain this statement, it may be useful, for the first time in this paper, to forget all physics and treat the simulation of the transport process as a black box. Each history run takes as input the initial position of the particle, always in phase space, and produces a distribution of estimator values depending on the outcome of some random numbers. Thus, the mean of all collected estimators is representative of the correlated quantity (i.e. the collision estimator can be defined in different ways to compute  $\phi(\vec{r}, E)$  or  $K_{eff}$ ). Thus, if the phase space is defined only in terms of a 1D space and energy, the estimator will be a  $N \times M$  matrix, where  $N$  and  $M$  are the dimensions of the vectors generated from the space and energy discretisation. The direct consequence is that when  $H$  histories are performed, the entire collection of data to be processed is a  $N \times M \times H$  matrix.

The Welford algorithm [15] is an on-line procedure capable of constructing mean and variance with only a single access to the single result of the random variable. This useful feature avoids the need to store the entire collection of estimators, as the mean and variance are updated as the random variable is generated. Thus, the

memory required is reduced to just three  $N \times M$  matrices: the estimator, the mean and the variance. A generic implementation is shown below.

*i)* collect  $x_n$  for all  $n = 1, \dots, N$

*ii)*  $\Delta = x_n - \bar{x}_{n-1}$

*iii)*  $\bar{x}_n = \bar{x}_{n-1} + \frac{\Delta}{n}$

*iv)*  $\Delta_2 = x_n - \bar{x}_n$

*v)*  $M_n^2 = M_{n-1}^2 + \Delta \cdot \Delta_2$

*vi)* return  $\bar{x} = \bar{x}_N$  and  $\sigma^2 = \frac{M_N^2}{N}$ .

This routine calculates the mean and variance after  $N$  histories.

# Chapter 5

## Code verification

### 5.1 Problem definition

This section presents a small verification campaign performed on the code described above. The case study is known as the slowing down problem or Placzek problem. The main advantage is that both the direct and adjoint cases allow an analytical solution, making the definition of a benchmark very accessible. They can be referred to as the Placzek function [16] and the adjoint Placzek function [12].

Consider an infinite homogeneous medium consisting of a single isotope, characterised by zero probability of particles being absorbed,  $\Sigma_a(E) = 0 \forall E$ . In this simplified case, the neutron transport equation can be written as

$$\Sigma_s(E)\phi(E) = \int_0^\infty \Sigma_s(E')f_s(E \rightarrow E')\phi(E')dE' + S(E) \quad (5.1)$$

where  $S(E)$  is a generic source term. Note that since the absorption cross section is zero, the fission cross section must also be zero. Now reduce the interactions to elastic and isotropic scattering only, recalling the equation (3.19)

$$\Sigma_s(E)\phi(E) = \int_E^{\frac{E}{\alpha}} \Sigma_s(E')\phi(E')\frac{dE'}{(1-\alpha)E'} + S(E). \quad (5.2)$$

This formulation highlights the fact that in this model neutrons can only jump within a limited energy range. In other words, neutrons can't lose more than a fraction  $\alpha$  of their own energy. The final simplification concerns the source term: considering most of the available neutron sources (i.e. the fission process), it is reasonable to

restrict the discussion, without loss of generality, to monochromatic sources only,  $S(E) = S\delta(E - E_0)$ , where  $\delta(x_0)$  is the Dirac's delta and  $E_0$  indicates the emission energy of the monochromatic source. The equation derived is

$$\Sigma_s(E)\phi(E) = \int_E^{\frac{E}{\alpha}} \Sigma_s(E')\phi(E') \frac{dE'}{(1-\alpha)E'} + S\delta(E - E_0). \quad (5.3)$$

It is more common to find it expressed in terms of collision density and as a function of the lethargy variable:  $u = -\ln\left(\frac{E}{E_0}\right)$ .

$$F(u) = \int_{u-\epsilon}^u \frac{e^{-(u-u')}}{1-\alpha} F(u') du' + S\delta(u). \quad (5.4)$$

Where  $\epsilon = \ln\left(\frac{1}{\alpha}\right)$ . The main difference is that negative motions in the energy domain correspond to positive motions in the lethargy domain. This is the main reason why the integral is defined only for lethargy values lower than the observed one, it automatically follows that the source is located at  $u = 0$ . It is obvious that the equation (5.4) is singular at  $u = 0$ , so the standard procedure is to treat the point separately.

$$F_0 = S. \quad (5.5)$$

However, it makes more sense to concentrate on the collision part. To solve the equation (5.4), note that each interval depends only on the previous one: it is possible to divide the lethargy domain into intervals such that  $(n-1)\epsilon < u < n\epsilon$ , so the equation (5.4) can also be constructed step by step. This useful property derives from the formulation of the scattering function, since it is impossible for a particle to pass between two non-contiguous intervals with a single interaction. The same discussion can be carried out by narrowing down around the source: neglecting the point  $u = 0$ , where the flux is infinite, and focusing on the first collision interval, it is possible to define a fictitious source term. This will be nothing more than the distribution of the particle after the first collision.

$$F_c(u) = \int_{u-\epsilon}^u \frac{e^{-(u-u')}}{1-\alpha} F_c(u') du' + Sf(0 \rightarrow u). \quad (5.6)$$

The general form of the collision kernel is retained to stress the physical meaning behind. Note that due to this simplification, the equation domain no longer resolves to  $u = 0$ . For convenience, the solution of the equation (5.6) is given in the book by

Montagnini [17]. The first two functions are reported as follows:

$$F_1(u) = S \frac{e^{(\frac{\alpha}{1-\alpha})u}}{1-\alpha}, \quad (5.7)$$

$$F_s(u) = S \left( \frac{1 - \alpha^{\frac{1}{1-\alpha}}}{1-\alpha} \right) e^{(\frac{\alpha}{1-\alpha})u} - S \left( \frac{1 - \alpha^{\frac{\alpha}{1-\alpha}}}{(1-\alpha)^2} \right) \left( u - \ln \left( \frac{1}{\alpha} \right) \right) e^{(\frac{\alpha}{1-\alpha})u}. \quad (5.8)$$

These are the most relevant because, as the particles move forward from the source position, they tend to forgive the initial distribution properties: the value of the Placzek function stabilises in  $F(u \gg 0) = S \left( 1 + \frac{\alpha}{1-\alpha} \ln \alpha \right)$ .

## 5.2 Direct Placzek problem

The figures 5.1, 5.4, 5.2, 5.5, 5.3 and 5.6 compare the equations (5.7) and (5.8) with the results of MC simulations carried out for different atomic numbers:  $A = 5, 8, 10, 15, 20, 25$  respectively. In all cases  $N = 10^5$  stories are performed and the means are coupled with a  $\pm 3\sigma$  confidence interval. The lethargy variable is plotted on the horizontal axis, while the collision density is plotted on the vertical axis,  $F(u) = \Sigma_t(u)\phi(u)$ . Lethargy and atomic number are thus the only independent variables analysed, as the Placzek function formulation for the collision density is independent of the material cross section.

Since the collision density is the quantity to be estimated, the collision estimator is applied without cross section correction, equation (4.19). This reduces the post-processing section to normalisation to the energy interval only and increases the accuracy of the code. A good agreement between the analytical solution and the stochastic solution can be observed, with almost no outliers. Another important point is that all characteristic discontinuities are well marked.

One fundamental observation is still missing: there are no negative lethargy values on the  $\vec{x}$  axis. The reason lies in the physics of the problem: since the defined scattering function does not include upscattering, no particles can be found at energy levels higher than that of the source. The source level is also neglected. An argument that differs from the correction applied when solving the simplified trans-

port equation can be attributed to the statistical nature of MC simulations: given a continuous random variable, the probability that it will take exactly a certain value is always identically zero. Applying this to the problem, it can be stated that after the first collision, no particle will have the exact initial energy, and for all subsequent events this point will be outside the result domain.

The last feature to be described is the asymptotic behaviour. The part of the curve defined along  $u < 3\epsilon$  takes the name of Placzek transients, because they are oscillations that become smoother with higher lethargy values. Again, the reason lies in the problem statistics: since the neutron property depends only on the previous state, the particle tends to forget the source distribution after a sufficiently large number of interactions. Phenomena that respect this constraint are called Markovian random walks. Consequently, only high energy levels are affected by the source, while the tail represents a continuous and homogeneous flux of particles.

### 5.3 Adjoint Placzek problem

The adjoint version of the equation (5.1) reads

$$\Sigma_s(E)\phi^\dagger(E) = \int_0^\infty \Sigma_s(E)f_s(E \rightarrow E')\phi^\dagger(E')dE' + S^\dagger(E). \quad (5.9)$$

Since this equation admits an analytical solution, it is not necessary to introduce adjoint cross sections and collision kernels. This is a useful point to emphasise the fact that, since the unknown is the adjoint flux and not the importance, any discussion of adjointons and their interactions is a purely mathematical game. The change on the 'direction' of the collision kernel has been done only to make the equation 3.2 solvable by MC codes. The distance is even greater when, as in this case, two different equations are being solved: whereas in solving the direct problem the aim is to check that the code output is consistent with the theoretical formulation, here the aim is to show that the solution of the pseudo transport equation (3.8) is consistent with the real one. Therefore, the formulation of the Placzek adjoint function is presented, imposing the equation (3.19). Thus, introducing the elastic

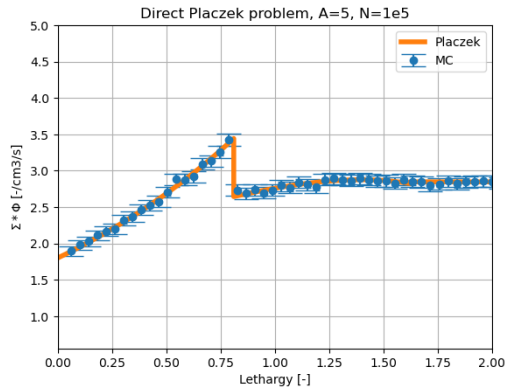


Figure 5.1: Analytical and simulated results of direct slowing down problem,  $A=5$ ,  $N=10^5$

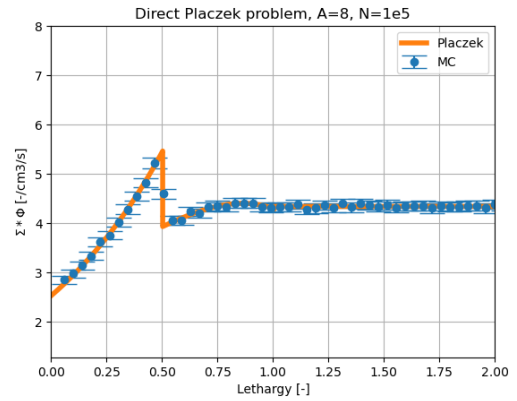


Figure 5.4: Analytical and simulated results of direct slowing down problem,  $A=8$ ,  $N=10^5$

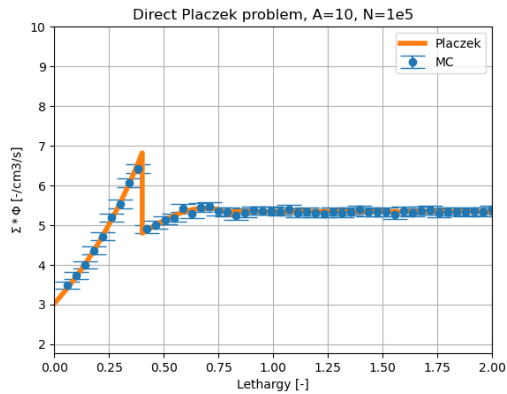


Figure 5.2: Analytical and simulated results of direct slowing down problem,  $A=10$ ,  $N=10^5$

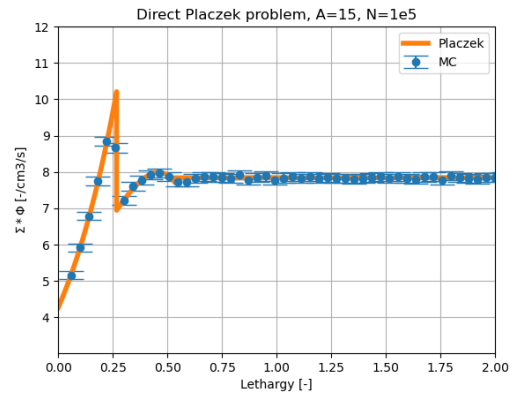


Figure 5.5: Analytical and simulated results of direct slowing down problem,  $A=15$ ,  $N=10^5$

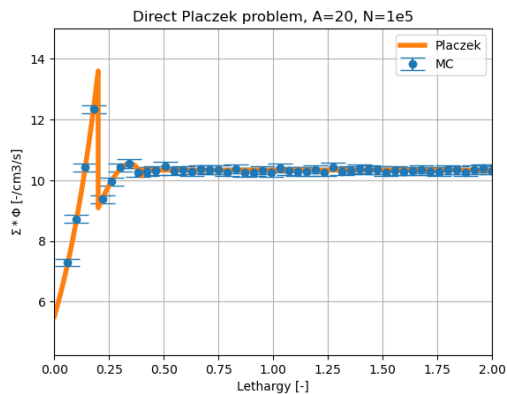


Figure 5.3: Analytical and simulated results of direct slowing down problem,  $A=20$ ,  $N=10^5$

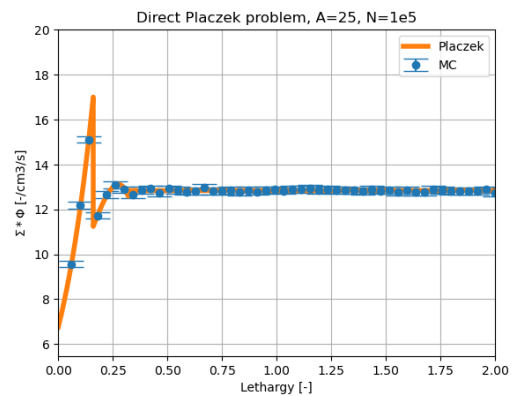


Figure 5.6: Analytical and simulated results of direct slowing down problem,  $A=25$ ,  $N=10^5$

scattering transfer function and a monochromatic source

$$\Sigma_s(E)\phi^\dagger(E) = \Sigma(E)\frac{1}{(1-\alpha)E} \int_{\alpha E}^E \phi^\dagger(E')dE' + S^\dagger\delta(E - E_0). \quad (5.10)$$

The solution of this equation is reported in detail in the paper by Saracco et al.[12]. To give a general idea of the procedure, the function can again be split into a singular part and a collided part. The formulation of the former is simple

$$\phi_0^\dagger = \frac{S^\dagger}{\Sigma_s(E_0)}. \quad (5.11)$$

The adjoint Placzek function is given in terms of the adjoint flux to maintain the nomenclature used by the authors, and dependent on energy to have a clearer form. The collided part is again defined by properties for any interval  $\frac{E_0}{\alpha^{n-1}} < E < \frac{E_0}{\alpha^n}$ . The first two group formulations are given explicitly

$$\phi_1^\dagger(E) = \frac{1}{E_0\Sigma_s(E_0)(1-\alpha)} \left(\frac{E}{E_0}\right)^{\frac{\alpha}{1-\alpha}}, \quad (5.12)$$

$$\begin{aligned} \phi_2^\dagger(E) = & \frac{1}{E_0\Sigma_s(E_0)(1-\alpha)} \left(\frac{E}{E_0}\right)^{\frac{\alpha}{1-\alpha}} \\ & \times \left[ (1-\alpha) \left(1 - \alpha^{\frac{1}{1-\alpha}}\right) - \left(\alpha^{\frac{1}{1-\alpha}} \ln \frac{\alpha E}{E_0}\right) \right]. \end{aligned} \quad (5.13)$$

The figures 5.7, 5.10, 5.8, 5.11, 5.9 and 5.12 are again made overlapping the adjoint Placzek function and the results of MC simulations on the adjoint. Note that although the formulation of the adjoint Placzek function is given for the adjoint flux, the adjoint collision density is used as a benchmark. The reason is the same as for the direct case: the slope of the collision density is independent of the material cross section. This property is retained, although it is less evident in the mathematical formulation. With the same idea of making the results easily reproducible, the normalised energy is used as an independent variable. Obviously, the normalisation is carried out using as a reference value that which characterises the source. Hence, the function is normalised with respect to the dimensionless energy interval,  $\Delta E_m = \frac{E_{m,up} - E_{m,low}}{E_0}$ . For completeness, the step between the adjoint flux and the adjoint collision density is also given.

$$F_c^\dagger(e) = \Sigma_t(E)\phi_c^\dagger(E) \cdot E_0 \quad (5.14)$$

where  $e = \frac{E}{E_0}$ . An interesting feature is the relationship between the independent random variable used to express the direct and adjoint Placzek functions. The lethargy scale can be aligned to a normalised logarithmic scale, while the normalised energy is a linear scale; thus both expressions show the same behaviour. It can be verified that they retain the same property when switching between scales. In a few words, the properties of the direct Placzek function in the logarithmic scale are reproduced for the relative adjoint in the linear scale and vice versa.

This point leads to a deeper consideration of the differences between particle and relative Placzek problems. It has just been mentioned that the source of the direct problem acts as a detector of the adjoint, so the detector of the direct problem becomes the source of the adjoint. Meanwhile, the functions obtained as solutions of the equations (5.4) and (5.10) have the same mathematical structure for the source,  $S(E) = S\delta(E - E_0)$ . The direct consequence is that the two Placzek functions do not refer to the same system, even if the introduced hypothesis is the same. This last concept may not seem so straightforward, since the starting point of this section is the application of the adjoint operator definition to the direct slowing-down problem, but it can be clarified by paying attention to the order in which the assumptions are applied. The transition from the direct to the adjoint problem is made before the source definition, when no constraints were required. A more direct confirmation can be obtained by looking at the domain of existence: neutrons can only exist for  $E < E_0$ , while adjunctons exist for  $E > E_0$ .

MC simulations are performed with the same setup as defined for the direct case:  $N = 10^5$  histories with a  $\pm 3\sigma$  confidence interval. The integral to be computed is again the basic collision estimator, equation (4.19). As expected, the stochastic estimate of the collision density agrees almost perfectly with the reference solution. Recalling the equation (3.20), it can be observed that  $\nu_s(E)$  is proportional to the integration interval. However, the integral has to be calculated numerically, so ideal extremes may differ from the values used by the software. A similar argumentation is reported in the section 4.4. As the discretisation imposes a lower bound on the reading of the energy intervals, it may happen that a relatively small value is rounded up to the smallest applicable value. Hence,  $\alpha \rightarrow 1$  when  $A$  increases. This is done in order to get a correct reading of the global trend of the blue dots. A closer look reveals that the values obtained by the MC simulations are generally slightly

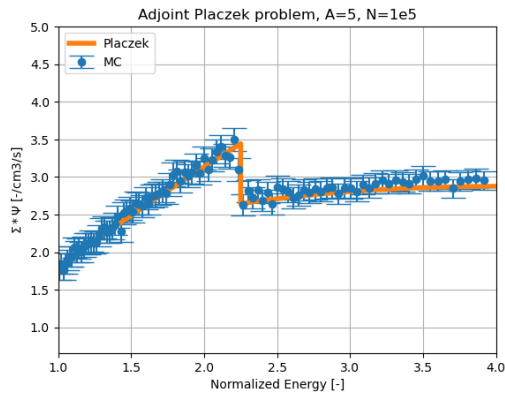


Figure 5.7: Analytical and simulated results of adjoint slowing down problem,  $A=5$ ,  $N=10^5$

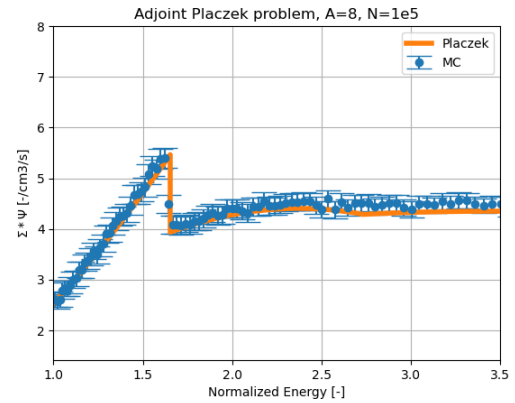


Figure 5.10: Analytical and simulated results of adjoint slowing down problem,  $A=8$ ,  $N=10^5$

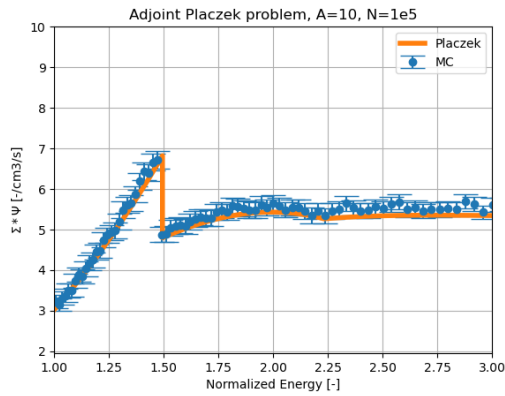


Figure 5.8: Analytical and simulated results of adjoint slowing down problem,  $A=10$ ,  $N=10^5$

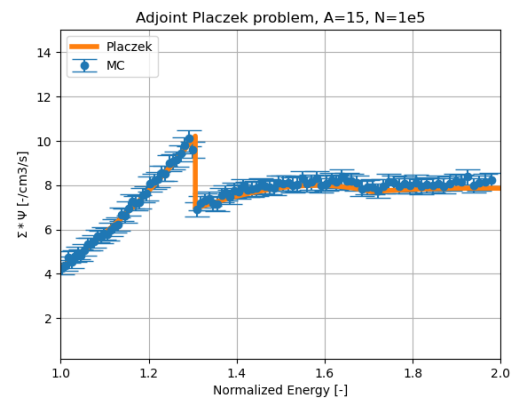


Figure 5.11: Analytical and simulated results of adjoint slowing down problem,  $A=15$ ,  $N=10^5$

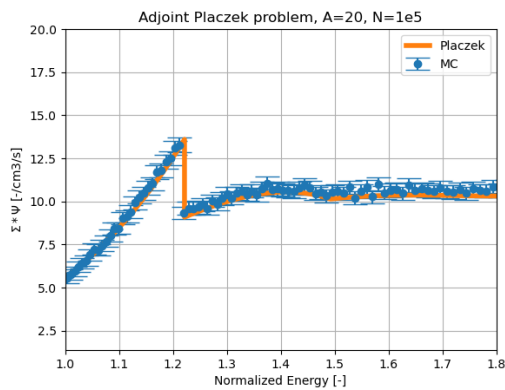


Figure 5.9: Analytical and simulated results of adjoint slowing down problem,  $A=20$ ,  $N=10^5$

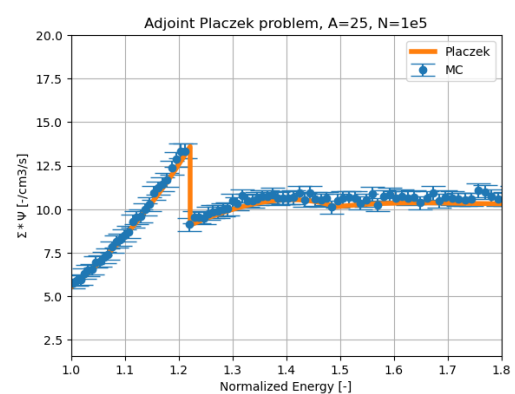


Figure 5.12: Analytical and simulated results of adjoint slowing down problem,  $A=25$ ,  $N=10^5$

higher than the Placzek function. Nevertheless, the numerical error introduced is less than the reported uncertainty and does not produce any outliers.

In equation (3.20), the cause of the increase of the statistical uncertainty can also be found. Especially for small values of  $A$ , the weight of the adjoints increases with each collision. In order to avoid an excessive impact on the reliability of the results, weight window technique is implemented. To sum up, the performance of the code is considered both satisfactory and reliable.

## 5.4 Statistical reliability of the results

The results of a MC code are represented by a collection of mean values and their associated uncertainty. The calculation of the uncertainty is based on the assumption of the validity of the Central Limit Theorem (CLT): assuming  $t$  run  $N$  stories

$$\sigma_{\bar{x}} = \frac{\sigma_x}{\sqrt{N}}. \quad (5.15)$$

Where  $x$  is a generic random variable to be sampled. The CLT, on the other hand, relies on the hypothesis that  $N$  is large enough to make the  $\bar{x}$  distribution converge to a Gaussian distribution. The value of  $N$  is not yet known. As mentioned in chapter 4, a common 'rule of thumb' suggests simulating at least 200 particles for each tally, however a more rigorous benchmark needs to be provided.

The analysis presented is based on the concept of Figure of Merit (FOM). It is a metric used to evaluate the efficiency of VR techniques and is defined as

$$FOM = \frac{1}{R_{\bar{x}}^2 T}. \quad (5.16)$$

Where  $R_{\bar{x}}$  is the relative standard deviation associated with the sample average's distribution, while  $T$  is the computational time required for the simulation. In short, it can be described as a compact form that takes into account both precision and computational cost: higher values of FOM indicate lower variance achieved in less time. The book by Haight [14] presents a useful approach aimed at checking the validity of the CLT by observing the FOM behaviour as a function of the number

of histories performed. The relative standard deviation can be expressed by the equation 5.15:

$$R_{\bar{x}} \approx \frac{\sigma_x}{\sqrt{N}} \approx \frac{C_1}{\sqrt{N}} \quad (5.17)$$

where  $C_1$  is a constant. It can also be assumed that the computation time increases linearly with the number of histories.

$$T \approx C_2 N. \quad (5.18)$$

It is therefore possible to write the FOM as a function of  $N$ .

$$FOM \approx \frac{1}{\left(\frac{C_1}{\sqrt{N}}\right)^2 C_2 N} \approx C. \quad (5.19)$$

The main corollary is that since  $R_{\bar{x}}$  is constructed from the equation 5.15, the validity of the CLT hypothesis can be confirmed by checking that the FOM fluctuates around a constant value.

In order to demonstrate that the applied algorithm follows the expected FOM behaviour, a series of simulations are carried out with different total numbers of particles:  $N = 2 \cdot 10^3, 5 \cdot 10^3, 10^4, 2 \cdot 10^4, 5 \cdot 10^4, 10^5$ . The case study considered is the adjoint Placzek problem in three different configurations:

- **reference**: no VR techniques applied;
- **weight window 1**: weight window technique is applied imposing  $w_{min} = 0.25$  and  $w_{max} = 2$ ;
- **weight window 2**: weight window technique is applied imposing  $w_{min} = 0.5$  and  $w_{max} = 4$ .

Two cases are studied for the application of the VR techniques, and since the FOM also allows to evaluate which configuration shows better performances, a small sensitivity analysis is carried out for the extremes of the weight window. It should be noted that some modifications are applied to the general FOM formula in order to adapt it to the data format. Since the result of the MC code is a vector representing the collision density distribution, the variance will also be the same, so the average variance value is used as a reference for the single simulation. Furthermore, the computation time is not expressed in standard units (i.e. seconds or minutes) as

it would be affected by machine performance. It is therefore decided to use the total number of random numbers generated to describe the computation time. This change can be made without loss of generality, since generating a random number is the most expensive among the basic operations performed during a Monte Carlo simulation. Finally, it is important to remember that both the relative standard deviations and the total random number generated are produced by an MC code, so they are random variables. To overcome this aspect and possible stochastic noise, the reported value is calculated as the mean between 20 identical simulations. Obviously, a correlated variance should also be reported in this case, but it would have become a self-perpetuating cycle. Therefore, since the objective of the study is only the global slope of the curve representing the FOM, the error bar is considered meaningless.

Figure 5.13 collects the results obtained by the simulations described. The small variations of the orange and green curves allow to assume that the convergence condition of the CLT is reached, but the analogue case appears more unstable. However, the most important information is the relative position between the curves. As mentioned above, higher FOM values mean higher efficiency. Thus, moving the allowed particle weight range upwards increases code performance. On the other hand, the application of VR techniques may be less effective at low particle numbers. In conclusion, an optimisation procedure may also be required for the application of VR techniques in order to maximise the efficacy.

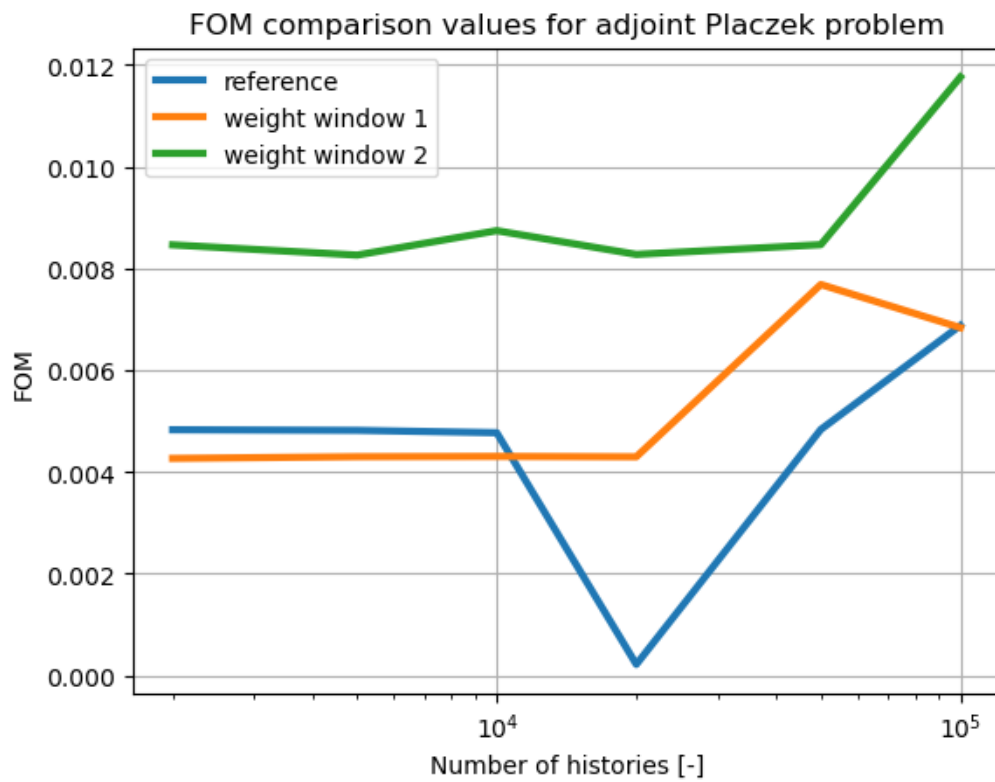


Figure 5.13: Comparison of FOM values for different weight windows

# Chapter 6

## Conclusions

MC methods are a fundamental tool in any nuclear application due to their extreme accuracy and ability to simulate very complex systems. On the other hand, they can require very intensive computational efforts to obtain acceptable results, but the increase in computational performance and the development of optimisation techniques make it possible to overcome this obstacle. This is how many MC codes were born and established themselves as reference tools for solving the Boltzman equation.

With the aim of applying standard stochastic methods to the solution of the importance equation, the formal definition of the adjoint operator is exploited. Once it is proven that the importance equation and the adjoint transport equation admit the same solution, it is possible to start from the latter and define a set of simulation rules to emulate the phenomena related to the importance balance equation. In this way, pseudo-particles and their transport properties, i.e., the adjoint cross section and the adjoint collision kernel, are introduced. A parallelism with neutrons led to the formalisation of these objects, called *adjunctons*. By imposing a correspondence between pairs of interactions, it is possible to derive the values of the adjoint properties from the direct ones, i.e. the neutron data libraries.

The characteristics of the new physical phenomena are therefore being studied in detail in order to gain a clear picture of the behaviour of the pseudoparticles.

An implementation procedure for a general MC transport code is proposed. Each step is carefully explained and potential problems are identified and addressed. Particular attention has been paid to the sampling of the source energy distribution of

the adjunctons: apart from the presence of a drastically different PDF, an optimised sampling procedure had to be developed due to the excessive computational time. The adaptation of the logarithmic rejection method to different isotopes is also presented. Following the events of a random walk, a useful discussion on the sampling of post-collision properties is carried out. Emphasis is placed on the multiplicity factor characteristic of adjoint scattering and how the numerical evaluation of integrals affects it. To conclude the description of the code, some VR and population control techniques are reported. Finally, the application of the collision estimator is reviewed.

After mapping the code structure, a verification campaign is carried out to test the reliability of the results. The slowing down problem is chosen as a benchmark because of the availability of an analytical solution, the Placzek function. A good agreement between the theoretical particle distribution and the simulation results is observed. The same set of experiments is applied to the adjoint case: also for this problem, the two solutions almost overlap.

Concerning the future perspectives for this work, the most straightforward step will be to carry out a verification campaign on a number of  $K$ -eigenvalue case studies. Although the present work includes the treatment of the fission term in both direct and adjoint transport, a meaningful collection of results should be produced and compared with benchmark cases available in the literature: tests aimed at replicating the Godiva reactor have already begun. After these preliminary verifications, the proposed approach could be applied in the framework of qualified industrial MC codes by introducing minor modifications to the algorithms already available and by preparing a set of modified nuclear data emulating the adjoint kernels. Once MC codes will be able to provide both direct and adjoint flux forms, a significant number of applications can be addressed using only stochastic approaches (i.e. reactor kinetic parameter evaluation). Zero-variance MC methods must be nominated, as it will be possible to develop an all-in-one code capable of first simulating adjoint transport and then using it to increase the accuracy of the direct simulation.

A more horizontal projection can be the study of alternative solutions for the construction of the total adjoint collision kernel. As has been widely discussed, the PDF to sample for the simulation of pseudoparticle random walks requires some optimi-

sations in order to reduce the simulation time. As an alternative to the equation (3.7), different assumptions can be introduced and tested to achieve better performance. Thus, although the use of the concept of importance is long established in nuclear engineering applications, stochastic solutions still have a huge and untapped potential to be explored in depth.

# Appendix A

## The adjoint operator

Let's introduce a generic function,  $f(\vec{x})$ , defined on a phase space with  $\vec{x}$  and an independent random variable. On the same domain, let's consider another function  $g(\vec{x})$  and an operator  $\theta$ . The adjoint operator of  $\theta$ , called  $\theta^\dagger$ , must respect the following equality

$$\int d\vec{x} g(\vec{x}), \theta f(\vec{x}) = \int d\vec{x} \theta^\dagger g(\vec{x}), f(\vec{x}). \quad (\text{A.1})$$

where  $\int d\vec{x}$  is the integral over the whole domain. It is also defined as inner products in phase space. An alternative notation is

$$(g(\vec{x}), \theta f(\vec{x})) = (\theta^\dagger g(\vec{x}), f(\vec{x})). \quad (\text{A.2})$$

In some cases it happens that  $\theta = \theta^\dagger$ , so the operator is defined as self-adjoint. Note that the adjoint condition is independent of the choice of functions  $f(\vec{x})$  and  $g(\vec{x})$ . The derivation of the adjoint transport equation is given. First, the scattering term:

$$\theta f(\vec{x}) = \oint_{4\pi} d\vec{\Omega}' \int_0^\infty dE' \Sigma_s(\vec{r}, E') f_s(\vec{r}, E', \vec{\Omega}' \rightarrow E, \Omega) \phi(\vec{r}, E', \vec{\Omega}'), \quad (\text{A.3})$$

$$g(\vec{x}) = \psi(\vec{r}, E, \vec{\Omega}), \quad (\text{A.4})$$

$$\begin{aligned} & (\psi(\vec{r}, E, \vec{\Omega}), \theta \phi(\vec{r}, E, \vec{\Omega})) = \\ & \int_V d\vec{r} \oint_{4\pi} d\Omega \int_0^\infty dE \psi(\vec{r}, E, \vec{\Omega}) \oint_{4\pi} d\vec{\Omega}' \int_0^\infty dE' \Sigma_s(\vec{r}, E') f_s(\vec{r}, E', \vec{\Omega}' \rightarrow E, \vec{\Omega}) \phi(\vec{r}, E', \vec{\Omega}'). \end{aligned} \quad (\text{A.5})$$

The passages are straightforward:  $\psi(\vec{r}, E, \vec{\Omega})$  can be moved inside the inner integral, since it does not depend on any variable to be integrated,  $d\vec{\Omega}' dE'$ , as a change of variable is performed  $(E', \vec{\Omega}') \longleftrightarrow (E, \vec{\Omega})$ . This can be done without any loss of completeness, since both variables are integrated over the whole domain. The result is

$$\begin{aligned} & (\psi(\vec{r}, E, \vec{\Omega}), \theta\phi(\vec{r}, E, \vec{\Omega})) = \\ & \int_V d\vec{r} \oint_{4\pi} d\vec{\Omega}' \int_0^\infty dE' \oint_{4\pi} d\vec{\Omega} \int_0^\infty dE \Sigma_s(\vec{r}, E) f_s(\vec{r}, E, \vec{\Omega} \rightarrow E', \vec{\Omega}') \psi(\vec{r}, E', \vec{\Omega}') \phi(\vec{r}, E, \vec{\Omega}), \end{aligned} \quad (\text{A.6})$$

$$\theta^\dagger \psi(\vec{r}, E, \vec{\Omega}) = \oint_{4\pi} d\vec{\Omega}' \int_0^\infty dE' \Sigma(\vec{r}, E) f_s(\vec{r}, E, \vec{\Omega} \rightarrow E', \vec{\Omega}') \psi(\vec{r}, E', \vec{\Omega}'). \quad (\text{A.7})$$

The derivation of the fission operator is neglected, since it is the same as the one just done. The only difference is that the collision kernel depends only on the outgoing energy,  $f_s(E) = \frac{\chi(E)}{4\pi}$ , so the operator is self-adjoint. So let's deal with the streaming term:

$$\theta f(\vec{x}) = \vec{\Omega} \cdot \nabla \phi(\vec{r}, E, \vec{\Omega}), \quad (\text{A.8})$$

$$(\psi(\vec{r}, E, \vec{\Omega}), \theta\phi(\vec{r}, E, \vec{\Omega})) = \int_V d\vec{r} \oint_{4\pi} d\vec{\Omega} \int_0^\infty dE \psi(\vec{r}, E, \vec{\Omega}) (\vec{\Omega} \cdot \nabla \phi(\vec{r}, E, \vec{\Omega})). \quad (\text{A.9})$$

Integration by parts must to be performed.

$$\begin{aligned} & \int_V d\vec{r} \oint_{4\pi} d\vec{\Omega} \int_0^\infty dE \psi(\vec{r}, E, \vec{\Omega}) (\vec{\Omega} \cdot \nabla \phi(\vec{r}, E, \vec{\Omega})) = \\ & \int_V d\vec{r} \oint_{4\pi} d\vec{\Omega} \int_0^\infty dE \nabla \cdot (\psi(\vec{r}, E, \vec{\Omega}) \vec{\Omega} \phi(\vec{r}, E, \vec{\Omega})) + \\ & - \int_V d\vec{r} \oint_{4\pi} d\vec{\Omega} \int_0^\infty dE (\vec{\Omega} \cdot \nabla \psi(\vec{r}, E, \vec{\Omega})) \phi(\vec{r}, E, \vec{\Omega}). \end{aligned} \quad (\text{A.10})$$

The first term can be simplified using the Gauss divergence theorem:

$$\begin{aligned} & \int_V d\vec{r} \oint_{4\pi} d\vec{\Omega} \int_0^\infty dE \nabla \cdot (\psi(\vec{r}, E, \vec{\Omega}) \vec{\Omega} \phi(\vec{r}, E, \vec{\Omega})) = \\ & = \int_{\delta V} dS \oint_{4\pi} d\vec{\Omega} \int_0^\infty dE \vec{n} \cdot \vec{\Omega} \psi(\vec{r}, E, \vec{\Omega}) \phi(\vec{r}, E, \vec{\Omega}). \end{aligned} \quad (\text{A.11})$$

In the majority of cases, void boundary conditions are applied, so that this term has become null.

$$(\psi(\vec{r}, E, \vec{\Omega}), \theta\phi(\vec{r}, E, \vec{\Omega})) = - \int_V d\vec{r} \oint_{4\pi} d\vec{\Omega} \int_0^\infty dE (\vec{\Omega} \cdot \nabla \psi(\vec{r}, E, \vec{\Omega}) \phi(\vec{r}, E, \vec{\Omega})), \quad (\text{A.12})$$

$$\theta^\dagger \psi(\vec{r}, E, \vec{\Omega}) = -\vec{\Omega} \cdot \nabla \psi(\vec{r}, E, \vec{\Omega}). \quad (\text{A.13})$$

# Bibliography

- [1] J. J. Duderstadt and W. R. Martin. *Transport Theory*. John Wiley & Sons, New York, 1979.
- [2] N. Metropolis and S. Ulam. The monte carlo method. *Journal of the American Statistical Association*, 44(247):335–341, 1949.
- [3] Nicholas Metropolis. The beginning of the monte carlo method. *Los Alamos Science*, 15:125–130, 1987.
- [4] E. Brun, F. Damian, C. M. Diop, E. Dumonteil, F. X. Hugot, C. Jouanne, Y. K. Lee, F. Malvagi, A. Mazzolo, O. Petit, J. C. Trama, T. Visonneau, and A. Zoia. Tripoli-4<sup>®</sup>: Cea, edf, and areva reference monte carlo code. *Annals of Nuclear Energy*, 82:151–160, 2015.
- [5] Jaakko Leppänen, M. Pusa, T. Viitanen, V. Valtavirta, and T. Kaltiaisenaho. The serpent monte carlo code: Status, development, and applications in 2013. *Annals of Nuclear Energy*, 82:142–150, 2015.
- [6] Paul K. Romano, Nicholas E. Horelik, Bryan R. Herman, Adam G. Nelson, Benoit Forget, and Kord Smith. Openmc: A state-of-the-art monte carlo code for research and development. *Annals of Nuclear Energy*, 82:90–97, 2015.
- [7] Alvin M. Weinberg and Eugene P. Wigner. *The Physical Theory of Neutron Chain Reactors*. The University of Chicago Press, Chicago, 1958.
- [8] Ussachoff and LN. Equation for the importance of neutrons, reactor kinetics and the theory of perturbations. In *Proc. Int. Conf. on the Peaceful Uses of Atomic Energy, Geneva, Switzerland, Aug. 8-21, 1955*, volume 5, pages 503–510, 1956.

- [9] J. Lewins. *Importance: The Adjoint Function - The Physical Basis of Variational and Perturbation Theory in Transport and Diffusion Problems*. Pergamon Press Ltd., London, 1965.
- [10] A. De Matteis. Phenomenological interpretation of the adjoint transport equation. *Meccanica*, 3:162–164, 1974.
- [11] A. De Matteis and R. Simonini. A new monte carlo approach to the adjoint boltzmann equation. *Nuclear Science and Engineering*, 65:93–164, 1978.
- [12] P. Saracco, S. Dulla, and P. Ravetto. The adjoint neutron transport equation and the statistical approach for its solution. *The European Physical Journal Plus*, 131(412), 2016.
- [13] V. Vitali, S. Dulla, P. Ravetto, and A. Zoia. Comparison of monte carlo methods for adjoint neutron transport. *The European Physical Journal Plus*, 133(8):317, 2018.
- [14] A. Haghigat. *Monte Carlo Methods for Particle Transport*. CRC Press, Boca Raton, 2021.
- [15] B. P. Welford. Note on a method for calculating corrected sums of squares and products. *Technometrics*, 4(3):419–420, 2012.
- [16] G. Placzek. On the theory of the slowing down of neutrons in heavy substances. *Physical Review*, 69:423–438, 1946.
- [17] B. Montagnini. Notes on reactor physics. Unpublished manuscript.